Neuroscience

Muscle-resident mesenchymal progenitors sense and repair peripheral nerve injury via the GDNF-BDNF axis

Reviewed Preprint
v1 • June 4, 2024
Not revised

Kyusang Yoo, Young-Woo Jo, Takwon Yoo, Sang-Hyeon Hann, Inkuk Park, Yea-Eun Kim, Ye Lynne Kim, Joonwoo Rhee, In-Wook Song, Ji-Hoon Kim, Daehyun Baek, Young-Yun Kong

School of Biological Sciences, Seoul National University, Seoul 08826, Republic of Korea • Molecular Recognition Research Center, Korea Institute of Science and Technology, Seoul 02792, Republic of Korea

Abstract

Fibro-adipogenic progenitors (FAPs) are muscle-resident mesenchymal progenitors that can contribute to muscle tissue homeostasis and regeneration, as well as postnatal maturation and lifelong maintenance of the neuromuscular system. Recently, traumatic injury to the peripheral nerve was shown to activate FAPs, suggesting that FAPs can respond to nerve injury. However, questions of how FAPs can sense the anatomically distant peripheral nerve injury and whether FAPs can directly contribute to nerve regeneration remained unanswered. Here, utilizing single-cell transcriptomics and mouse models, we discovered that a subset of FAPs expressing GDNF receptors *Ret* and *Gfra1* can respond to peripheral nerve injury by sensing GDNF secreted by Schwann cells. Upon GDNF sensing, this subset becomes activated and expresses *Bdnf*. FAP-specific inactivation of *Bdnf* ($Prrx1^{Cre}$; $Bdnf^{fl/fl}$) resulted in delayed nerve regeneration owing to defective remyelination, indicating that GDNF-sensing FAPs play an important role in the remyelination process during peripheral nerve regeneration. In aged mice, significantly reduced *Bdnf* expression in FAPs was observed upon nerve injury, suggesting the clinical relevance of FAP-derived BDNF in the age-related delays in nerve regeneration. Collectively, our study revealed the previously unidentified role of FAPs in peripheral nerve regeneration, and the molecular mechanism behind FAPs' response to peripheral nerve injury.

eLife assessment

This interesting study reports that muscle contains fibro-adipogenic progenitor cells (FAPs) that promote regeneration following injury of peripheral neurons. These novel results indicate that several known growth factors are involved in the process of regeneration. This is an **important** contribution, however the analysis is **incomplete** since additional experimental data is needed to support the main conclusions.

https://doi.org/10.7554/eLife.97662.1.sa3

Introduction

Positioned in the interstitial space between myofibers (Uezumi, et al., 2010), fibro-adipogenic progenitors (FAPs) interact with cellular components within skeletal muscle to ensure normal development, homeostasis, and regeneration of muscle tissue. During developmental myogenesis, embryonic FAPs expressing *Osr1* contribute to limb muscle patterning by regulating the expression of extracellular matrix (ECM) genes that make up muscle connective tissue (Vallecillo-Garcia, et al., 2017). In young adults, FAPs are necessary for normal growth and long-term maintenance of skeletal muscle, which otherwise undergo progressive muscle atrophy in the absence of PDGFRα^{+} FAPs (Roberts, et al., 2013; Wosczyna, et al., 2019; Uezumi, et al., 2021). Upon muscle injury, FAPs proliferate in response to IL-4/IL-13 signals from eosinophils, and participate in clearing of necrotic debris via phagocytosis (Heredia, et al., 2013). Also, the proliferated FAPs regulate expansion and asymmetric commitment of muscle stem cells (MuSCs) via secreted factors such as WISP1, leading to robust *de novo* myofiber formation (Joe, et al., 2010; Lukjanenko, et al., 2019; Wosczyna, et al., 2019). Conversely, absence of FAPs or its functional decline with age cause premature differentiation of MuSCs upon injury, resulting in formation of smaller regenerated myofibers (Murphy, et al., 2011; Lukjanenko, et al., 2019; Wosczyna, et al., 2019). After sufficient regeneration of myofibers occurs, FAPs undergo apoptosis via TNF signaling from monocyte/macrophages, such that its numbers return to those of unperturbed muscles (Lemos, et al., 2015; Saito, et al., 2020). Failure to remove excess FAPs after muscle regeneration results in unwanted fibrosis, which compromises muscle function (Uezumi, et al., 2011; Uezumi, et al., 2014).

In addition to formation and maintenance of muscle tissue, FAPs also contribute to maturation and maintenance of the neural components within skeletal muscle. Previously, we reported that FAPs promote postsynaptic maturation of the neuromuscular junction (NMJ) through the BAP1/SMN axis during postnatal development (Kim, et al., 2022). Selective inactivation of *Bap1* in FAPs results in dysfunctional NMJs, with sustained expression of the immature form of acetylcholine receptor subunit, *AchRγ*, in skeletal muscle (Kim, et al., 2022). Progressively, these mice exhibit denervation at the NMJ, retraction of motor axons, reduction of myelination and axon diameter, and eventually motor neuron loss, suggesting that FAPs prevent the dying-back loss of motor neurons (Kim, et al., 2022). Recently, we also reported defective presynaptic maturation and maintenance in mice with selective *Smn* downregulation in FAPs, again suggesting the role of FAPs in postnatal NMJ development (Hann, et al., 2023). In adult mice, BMP3B secretion by FAPs stabilize NMJs and Schwann cells by promoting the myelination program in Schwann cells, thereby directly contributing to the maintenance of neural components within skeletal muscle (Uezumi, et al., 2021). In the absence of FAPs or *Bmp3b*, mice exhibit muscle weakness and myofiber atrophy along with destabilization of Schwann cells and denervation at NMJs, which closely resemble the phenotypes observed in age-related sarcopenia (Uezumi, et al., 2021). Similarly, conditional deletion of *Bap1* in FAPs in adulthood cause denervation at the NMJs and eventually loss of motor neurons, demonstrating the requirement of FAPs in maintaining the neuromuscular system (Kim, et al., 2022). Conversely, disturbance in the neural component can influence the behavior of FAPs; for instance, denervation is known to activate FAPs (Contreras, et al., 2016; Gonzalez, et al., 2017; Madaro, et al., 2018). This suggests that FAPs can somehow sense the anatomically distant peripheral nerve injury. However, the question of how FAPs are able to sense the distant peripheral nerve injury remains unanswered (Theret, et al., 2021). Furthermore, whether FAPs are actually able to exert beneficial effects on peripheral nerve regeneration remains elusive.

In accordance with its various functions, heterogeneity within FAPs began to be recognized with the advent of single-cell analysis technology (Contreras, et al., 2021). By profiling the expression levels of 87-selected genes in isolated singlets of FAPs, dynamic transitions between heterogeneous

subpopulations of FAPs, identified by different expression levels of TIE2 and VCAM1, was observed during postnatal and regenerative myogenesis (Malecova, et al., 2018). The report showed that while activation of TIE2^{high} FAPs is observed in neonatal mice, activation of VCAM1^{+} FAPs is observed in injured muscles, suggesting distinct functional involvement of FAPs in the two different contexts of myogenesis (Malecova, et al., 2018). Additionally, single-cell RNA-sequencing (scRNA-seq) enabled identification of heterogeneity within FAPs based on the genome-wide transcriptome data (Lieberman, et al., 2021). In homeostatic adult muscle, two distinct subpopulations within FAPs have been identified, namely *Dpp4*$^{+}$ and *Cxcl14*$^{+}$ FAPs (Scott, et al., 2019; Oprescu, et al., 2020). Functionally, we reported that DPP4^{+} FAPs contribute to maturation and maintenance of the neuromuscular system via the BAP1/SMN axis (Kim, et al., 2022). In juvenile muscle, five different subpopulations within FAPs were characterized, each having different contexts of activation and differentiation potentials (Leinroth, et al., 2022). *Osr1*$^{+}$ FAPs are precursor cells that can form all other subpopulations; *Clu*$^{+}$ FAPs are most potent in mineralization; *Adam12*$^{+}$ and *Gap43*$^{+}$ FAPs are immune-responsive; and *Hsd11b1*$^{+}$ FAPs respond to nerve transection (Leinroth, et al., 2022). The different activation cues and differentiation potentials in each subpopulation of FAPs suggest distinct roles those subsets can play in different contexts of skeletal muscle biology. Indeed, dynamic transcriptomic changes in FAP subpopulations in response to muscle injury (Scott, et al., 2019; De Micheli, et al., 2020; Oprescu, et al., 2020) or denervation (Nicoletti, et al., 2020; Proietti, et al., 2021; Lin, et al., 2022; Nicoletti, et al., 2023) have been identified in studies that implemented scRNA-seq analysis. Still, the question of how FAPs may sense the distant nerve injury and whether FAPs can beneficially contribute to nerve regeneration remain largely unknown.

Here, using the scRNA-seq approach, we aimed to identify the response mechanism of FAPs to nerve injury, by uncovering its nerve injury-sensing mechanism and its potentially beneficial effect on nerve regeneration. To obtain a comprehensive scRNA-seq database of FAPs' response to nerve injury, FAPs from both chronic, non-regenerating nerve injury (denervation)- and acute, regeneration-prone nerve injury (crush)-affected muscles were collected at different time points over the course of regeneration. As a result, distinct transcriptomic profiles of FAPs at different time points post the two types of nerve injuries were captured in single-cell resolution, from which the response mechanism of FAPs to nerve injury was identified and validated using mouse models. Specifically, we found that upon peripheral nerve injury, GDNF from Schwann cells can activate FAPs, which in turn express BDNF to promote remyelination during nerve regeneration. Our study suggests FAPs as an important player that actively participates in the nerve regeneration process, of which we believe should be considered in future studies aiming for improved understanding of the peripheral nerve regeneration process.

Results

Distinct response profiles of FAPs upon nerve crush injury versus denervation

To establish a comprehensive transcriptome database of nerve injury-affected FAPs at single-cell resolution, we performed scRNA-seq using FAPs isolated from sciatic nerve crush injury (SNC)- or denervation (DEN)-affected muscles at different time points over the course of regeneration (**Figure 1—figure supplement 1A** and **B**). Four time points (3, 7, 14, and 28 days post injury, hereafter dpi) along the regeneration process were chosen for analysis to capture the transcriptomes of FAPs at both early and late stages of regeneration. Selection of such time points was based on a previous report that showed the reinnervation process of the tibialis anterior (TA) muscle after SNC, where Wallerian degeneration was evident at 7 dpi, and reinnervation was mostly completed at 28 dpi (Magill, et al., 2007). Including the uninjured control, scRNA-seq data from a total of nine samples (Uninjured, SNC-3dpi, SNC-7dpi, SNC-14dpi, SNC-28dpi, DEN-3dpi, DEN-7dpi, DEN-14dpi, and DEN-28dpi) were obtained via the 10x Genomics platform (**Figure 1—**

figure supplement 1A). Quality control and filtering of the sequenced cells yielded a total of 44,597 cells for further analysis, where 4955.2±1022.8 cells were captured from each sample. Prior to downstream analysis, integration (Hao, et al., 2021) of our scRNA-seq data with a publicly available scRNA-seq data of mononuclear cells from denervated muscles at 0, 2, 5, and 15 dpi (Nicoletti, et al., 2023) was carried out for data validation. Expectedly, most (97.7%) of the filtered cells in our scRNA-seq data clustered with the denervation-affected FAPs in the published scRNA-seq data, confirming the validity of the data produced in our study (**Figure 1—figure supplement 1C** and **D**).

To look into the chronological transcriptomic changes that occur in FAPs in response to SNC or DEN on a global level, we analyzed our scRNA-seq data by samples. Visualization of the scRNA-seq data on uniform manifold approximation and projection (UMAP) plots showed similar changes in the early stages of regeneration (3 and 7 dpi) compared to uninjured FAPs, regardless of the type of injury (**Figure 1A**). However, as FAPs reached later stages of regeneration (14 and 28 dpi), SNC-affected FAPs returned to states similar to uninjured control, while DEN-affected FAPs stayed in the activated state (**Figure 1A**). The similarities and differences observed on the UMAP plots could also be found in the differentially expressed gene (DEG) analyses as well as in the hierarchical clustering analysis using those DEGs (**Figure 1B–E**, **Figure 1—figure supplement 2A–C**). As a result of pairwise DEG analyses comparing all nine samples, different numbers of DEGs were identified, of which correlated with the similarities between samples observed on UMAP plots (**Figure 1A–E**, **Figure 1—figure supplement 2A** and **B**). Hierarchical clustering of the nine samples using all unique DEGs identified from the pairwise comparisons showed clustering of uninjured control with SNC-14dpi and SNC-28dpi, suggesting FAPs' return to homeostatic state (**Figure 1—figure supplement 2C**). On the other hand, DEN-14dpi and DEN-28dpi clustered with each other, but not with uninjured control, suggesting the chronic activation of FAPs in response to DEN as reported previously (Madaro, et al., 2018) (**Figure 1—figure supplement 2C**). Samples that captured the early responses of FAPs to nerve injuries (3 or 7 dpi) were clustered together by dpi rather than the type of injury, suggesting similar response profiles of FAPs to both types of nerve injuries (**Figure 1—figure supplement 2C**). Indeed, the numbers of DEGs between SNC-3dpi versus DEN-3dpi and SNC-7dpi versus DEN-7dpi were among the lowest identified in the pairwise analyses (**Figure 1B** and **C**, **Figure 1—figure supplement 2A**). Overall, the number of DEGs between SNC- and DEN-affected FAPs increased significantly with dpi, showing the bifurcation of FAP's response to the different types of nerve injuries in the later stages of regeneration (**Figure 1B–E**).

In a previous study, chronic activation of the STAT3/IL-6 pathway in FAPs in response to DEN was reported (Madaro, et al., 2018). Indeed, *Il6* was identified as one of the genes upregulated at all four time points in response to DEN compared to uninjured control in our data (**Figure 1—figure supplement 2D** and **E**). Although it did not pass the fold change (FC) threshold (FC >= 2) in the DEG analyses, expression of *Stat3* also showed significant chronic upregulation in all DEN-affected FAPs as well (**Figure 1—figure supplement 2F** and **G**). In response to SNC, however, only transient upregulation of both genes was observed (**Figure 1—figure supplement 2D–G**).

To obtain biological insights on the different responses of FAPs to SNC versus DEN in the later stage of regeneration, we subjected the two lists of genes from **Figure 1E** (28 dpi, SNC_UP and DEN_UP) to gene set overrepresentation analysis (ORA) using g:Profiler (Kolberg, et al., 2023). From both sets of genes, pathways related to tissue regeneration/wound healing were enriched (**Figure 1F** and **G**, **Figure 1—figure supplement 3A** and **B**). In contrast, pathways related to immune cell recruitment, inflammation, and ECM regulation by collagen biosynthesis were enriched specifically in DEN-28dpi (**Figure 1F**, **Figure 1—figure supplement 3A**), which is consistent with the previous report that showed the direct contribution of FAPs to fibrosis in denervated muscles (Contreras, et al., 2016; Madaro, et al., 2018). Also, mild immune cell infiltration into affected muscles in response to DEN was previously described (Lin, et al., 2022; Nicoletti, et al., 2023); our results suggest the role of FAPs in chemotactic recruitment of immune

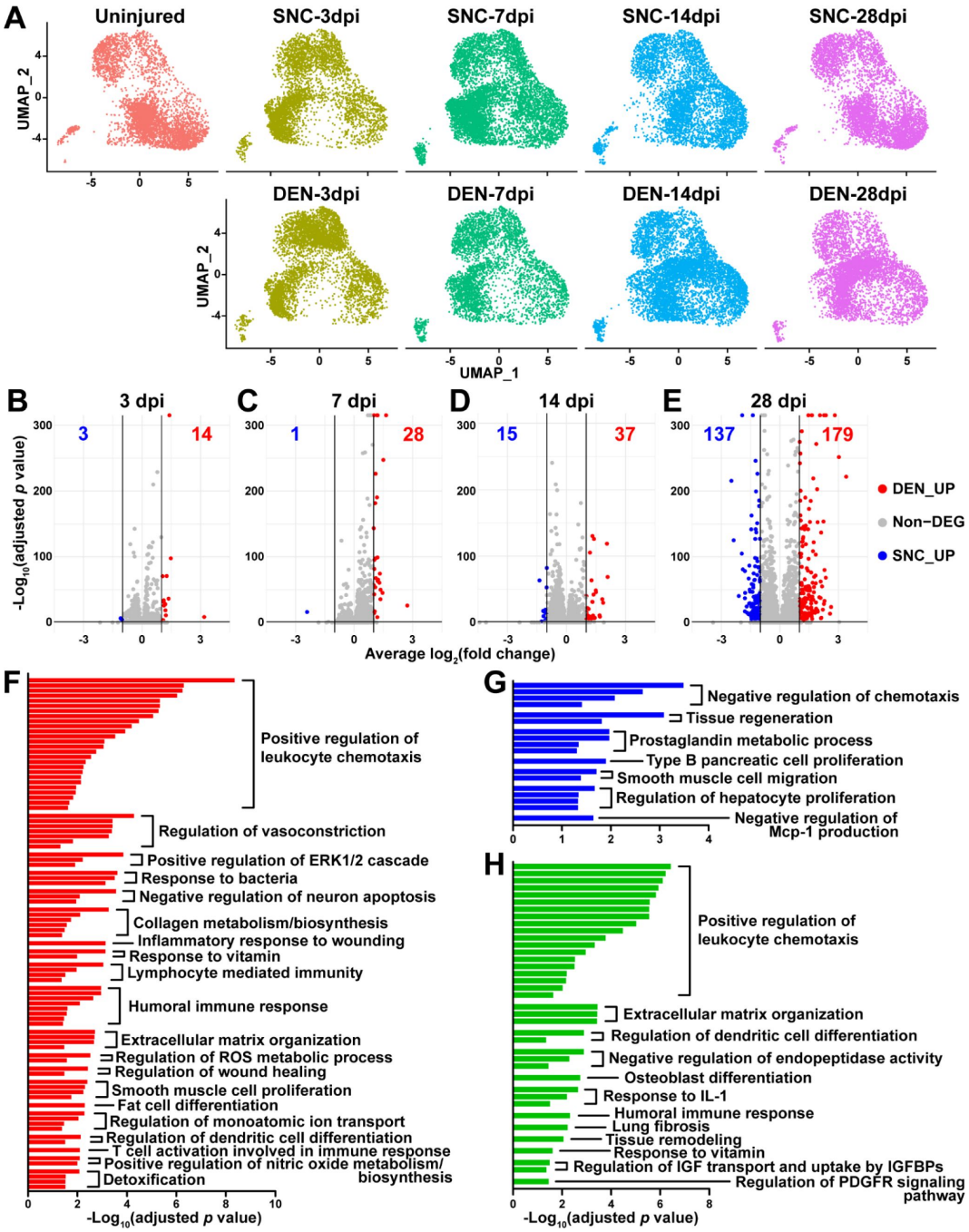

Figure 1.

Distinct response profiles of FAPs upon nerve crush injury versus denervation

(**A**) Single-cell transcriptome data of nerve injury-affected FAPs displayed separately by samples on UMAP plots. (**B**–**E**) Volcano plots showing different numbers of DEGs identified from comparing SNC-vs DEN-affected FAPs at (B) 3, (C) 7, (D) 14, (E) 28 days post injury (dpi). (**F**–**H**) Pathway terms enriched from gene set overrepresentation analyses using g:Profiler. DEGs used as input were (F) DEN-28dpi-upregulated versus SNC-28dpi, (G) SNC-28dpi-upregulated versus DEN-28dpi, and (H) DEGs upregulated commonly in SNC-3dpi, SNC-7dpi, DEN-3dpi, and DEN-7dpi versus uninjured control.

cells in denervated muscles. In addition, the pathway 'negative regulation of neuron apoptosis' was enriched in DEN-28dpi, suggesting a prolonged attempt of FAPs to preserve neurons that must be alive for reinnervation of the denervated muscle (**Figure 1F**, **Figure 1—figure supplement 3A**). On the other hand, some pathways were exclusively enriched in SNC-28dpi, such as negative regulation of chemotaxis and prostaglandin metabolism (**Figure 1G**, **Figure 1—figure supplement 3B**). It is generally understood that after a successful tissue regeneration process, resolution of immune response allow for the tissue to return to homeostasis (Ortega-Gomez, et al., 2013; Aurora and Olson, 2014; Julier, et al., 2017); our results suggest the role of FAPs in regulating immune resolution near the end of nerve regeneration. Furthermore, the role of prostaglandin in peripheral nerve regeneration has recently been described (Forese, et al., 2020; Bakooshli, et al., 2023); our ORA results suggested that FAPs may also be involved in regulation of prostaglandin levels during peripheral nerve regeneration.

To discover biological pathways behind the supposedly similar responses of FAPs to both SNC and DEN in the early phases of regeneration, we examined DEGs from comparing SNC-3dpi, SNC-7dpi, DEN-3dpi, and DEN-7dpi to uninjured controls. Many of the upregulated genes identified in the DEG analyses were shared amongst the four samples (**Figure 1—figure supplement 3C**). ORA using the shared upregulated genes revealed enrichment in pathways that were also enriched in DEN-28dpi compared to SNC-28dpi, such as immune cell recruitment and ECM regulation, supporting the idea that early-activated states within FAPs persist for a prolonged period in response to DEN (**Figure 1F** and **H**, **Figure 1—figure supplement 3A** and **D**). Collectively, analysis of our scRNA-seq data by samples revealed similar response profiles of FAPs to both SNC and DEN in the early stages of regeneration, which then bifurcated into chronic activation in response to DEN and return to homeostasis in response to SNC, showing correlative behaviors along with the degree of nerve regeneration and target muscle reinnervation.

Nerve injury-responsive subsets within FAPs

Although analysis of our scRNA-seq data on the population level provided general insights on how FAPs may respond to the different types of nerve injuries, the results could not provide us with sufficient clues on how FAPs can sense nerve injuries, or how they may directly contribute to nerve regeneration. Thus, we next analyzed our scRNA-seq data on the subpopulation level, hoping to distinguish subsets within FAPs that may be more relevant to the context of sensing and responding to nerve injury. To identify distinct subsets within nerve injury-affected FAPs, we applied unsupervised clustering to the merged scRNA-seq data of all nine samples following the Seurat-R workflow (Hao, et al., 2021). As a result, seven clusters with unique gene expression profiles were identified from the nerve injury-affected FAPs, with marker genes specifically expressed in each cluster (**Figure 2A–C**, **Figure 2—figure supplement 1A**).

Interestingly, while clusters 4-7 showed little or no significant change in their proportions in response to nerve injury, clusters 1-3 exhibited dramatic changes upon nerve injury (**Figure 2D** and **E**). In particular, cluster 1 was mostly present in uninjured muscles or in muscles where reinnervation had occurred to at least some degree (SNC-14dpi and SNC-28dpi) (Magill, et al., 2007) (**Figure 2D** and **E**). In contrast, presence of clusters 2 and 3 were mutually exclusive to cluster 1, such that their appearances were transient in response to SNC and chronic upon DEN (**Figure 2D** and **E**). Based on this mutual exclusivity of the three clusters, we speculated that cluster 1 can sense and respond to nerve injuries, and that clusters 2 and 3 may have arisen from cluster 1 upon nerve injury.

To obtain clues on whether such changes between FAP clusters could have actually occurred in response to nerve injury, we first performed RNA velocity analysis using R package velocyto.R (La Manno, et al., 2018). RNA velocities on the UMAP plots predicted transcriptomic flow from cluster 1 to clusters 2 and 3 in the early stages of regeneration in both SNC- and DEN-affected FAPs, which was in line with our speculation (**Figure 2—figure supplement 1B**). Conversely, transcriptomic flow from clusters 2 and 3 back to cluster 1 was evident in SNC-affected FAPs in the

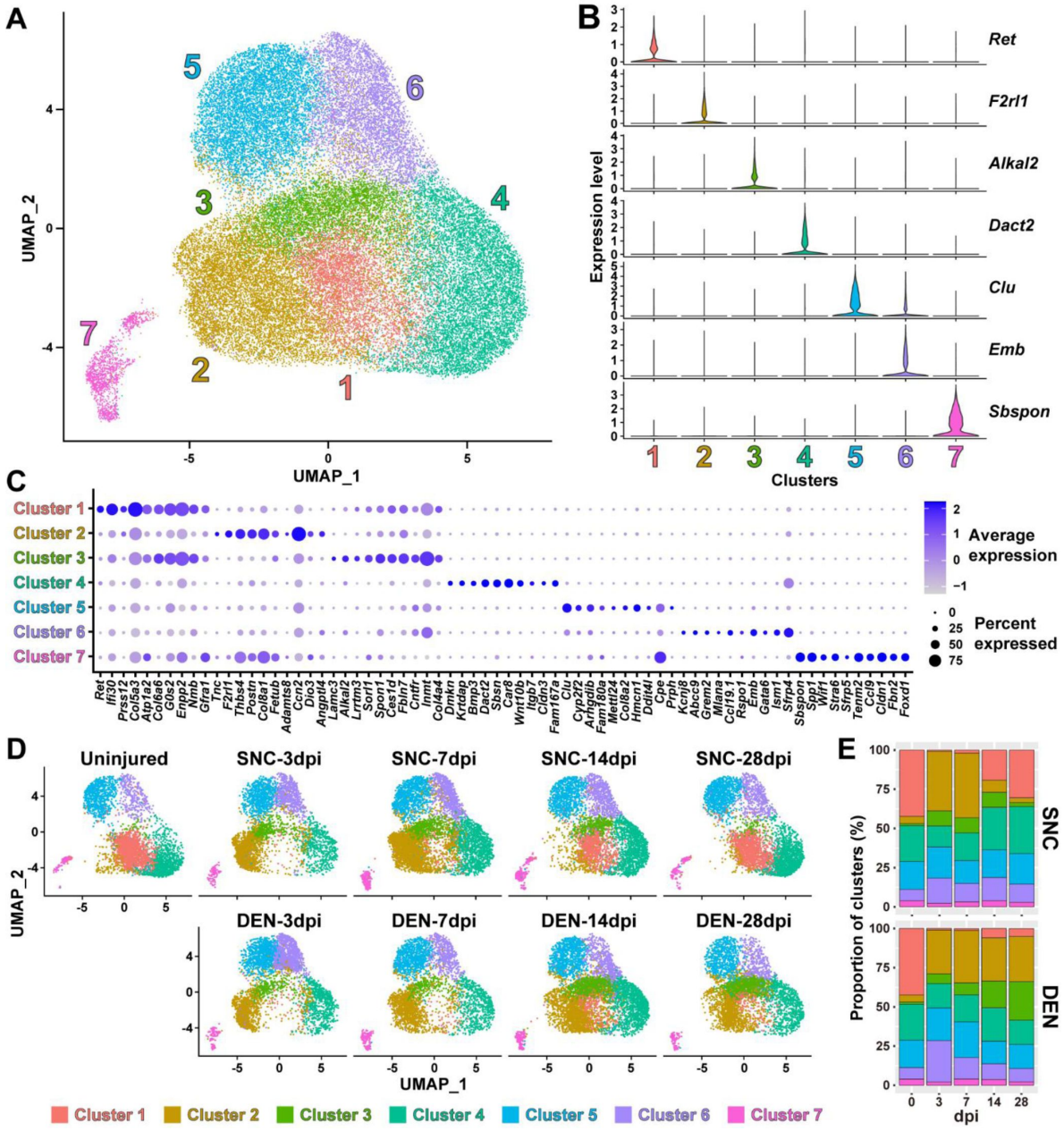

Figure 2.

Nerve injury-responsive subsets within FAPs

(**A**) Seven clusters identified by unsupervised clustering using all nine scRNA-seq samples obtained in this study displayed on the UMAP plot. (**B**) Violin plots showing expressions of unique marker genes identified in each cluster. (**C**) Dotplot showing the expression levels and percentages of top 10 DEGs enriched in each cluster. (**D**) UMAP plots of clustered scRNA-seq data displayed separately by samples. (**E**) Barplots showing the proportions of the seven clusters that comprise each scRNA-seq sample of nerve injury-affected FAPs. For 0 dpi, data from the same uninjured control sample is displayed for both SNC and DEN.

later stages of regeneration (**Figure 2—figure supplement 1B**). However, RNA velocities in DEN-affected FAPs were represented as dots instead of arrows on clusters 2 and 3 in the later stages, suggesting an unchanging, chronic state of their transcriptomes, which is consistent with the chronic activation of FAPs in response to DEN (Madaro, et al., 2018) (**Figure 2—figure supplement 1B**). Additionally, hierarchical clustering of the seven FAP clusters using DEGs enriched in each cluster grouped clusters 1-3 together, supporting our speculation that clusters 2 and 3 originate from cluster 1 (**Figure 2—figure supplement 1C**). Recently, *Hsd11b1*-expressing FAPs were identified as the FAP subset that is specifically activated in response to nerve transection injury (Leinroth, et al., 2022). Since we speculated that cluster 1 in our scRNA-seq data can sense and respond to nerve injury, we examined the expressions of marker genes identified in the previous report – *Hsd11b1*, *Mme*, *Ret*, and *Gfra1* (Leinroth, et al., 2022) – in our scRNA-seq data. Indeed, all four markers were enriched in cluster 1 in our data (**Figures 3A** and **B**, **Figure 2—figure supplement 1D–F**). Expressions of marker genes *Hsd11b1* and *Mme* were also enriched in clusters 2 and 3, further supporting the idea that those clusters may have arisen from cluster 1 (**Figure 2—figure supplement 1D–F**). Together, these data suggest that clusters 1-3 are the dynamic interchanging subsets of FAPs that specifically respond to nerve injury, where cluster 1 senses nerve injuries in unperturbed muscles and clusters 2 and 3 arise from cluster 1 to respond to nerve injury.

GDNF signaling pathway in the nerve injury-sensing mechanism by FAPs

Among the four marker genes expressed in cluster 1, *Ret* and *Gfra1* are well-known as GDNF receptors, where Gfra1 directly binds GDNF, which in turn activates the receptor tyrosine kinase (RTK) Ret for downstream signal transduction (Jing, et al., 1996; Treanor, et al., 1996; Trupp, et al., 1996). Meanwhile, robust but specific expression of GDNF by Schwann cells in response to peripheral nerve injury has been reported (Hammarberg, et al., 1996; Hoke, et al., 2002; Arthur-Farraj, et al., 2012; Xu, et al., 2013; Proietti, et al., 2021). Accordingly, we presumed that FAPs, especially the *Ret*- and *Gfra1*-expressing cluster 1 cells, may sense the distant nerve injury by detecting GDNF secreted from Schwann cells. Notably, both *Ret* and *Gfra1* were among the top 10 DEGs specifically enriched in cluster 1, suggesting that they can readily respond to GDNF (**Figure 2C**, **Figure 3—figure supplement 1A**). In addition, comparing the expression levels of *Ret* and *Gfra1* in skeletal muscle-resident mononuclear cell populations isolated by fluorescence-activated cell sorting (FACS) revealed robust co-expression of both genes in FAPs, but not as much in other cell populations (**Figure 3C** and **D**). Thus, FAPs may be the main cell type within skeletal muscle that can respond to GDNF secreted by Schwann cells in case of a nerve injury.

To further investigate the relevance of GDNF signaling in the nerve injury-sensing mechanism by FAPs, we subjected lists of DEGs enriched in clusters 1-3 to ORA. Genes enriched in cluster 1 returned pathways ‘GDNF receptor signaling pathway’, ‘regulation of cellular response to growth factor stimulus’, and ‘positive regulation of peptidyl-tyrosine phosphorylation’, where tyrosine residues on the RTK Ret is known to be phosphorylated upon activation (Jing, et al., 1996; Treanor, et al., 1996; Trupp, et al., 1996) (**Figure 3—figure supplement 1B**). The two latter pathways were also found in the ORA results using DEGs enriched in clusters 2 and 3, supporting the idea that those clusters originate from cluster 1 upon nerve injury (**Figure 3E**, **Figure 3—figure supplement 2A** and **B**). The pathway ‘positive regulation of ERK1/2 cascade’ was enriched in cluster 2, suggesting the involvement of GDNF-Ret-Ras-ERK signaling cascade within the MAPK signaling pathway in this cluster (Airaksinen and Saarma, 2002; Sariola and Saarma, 2003; Kanehisa, et al., 2023) (**Figure 3G**, **Figure 3—figure supplement 1C** and **2A**). In addition to ORA, we predicted upstream transcription factors (TFs) that could have regulated the expressions of the DEGs enriched in the two activated FAP subsets, clusters 2 and 3, using TRRUST (Han, et al., 2018). As a result, TFs *Fos*, *Jun* and *NF-κB* (*Nfkb1*, *Nfkb2*) were predicted from both

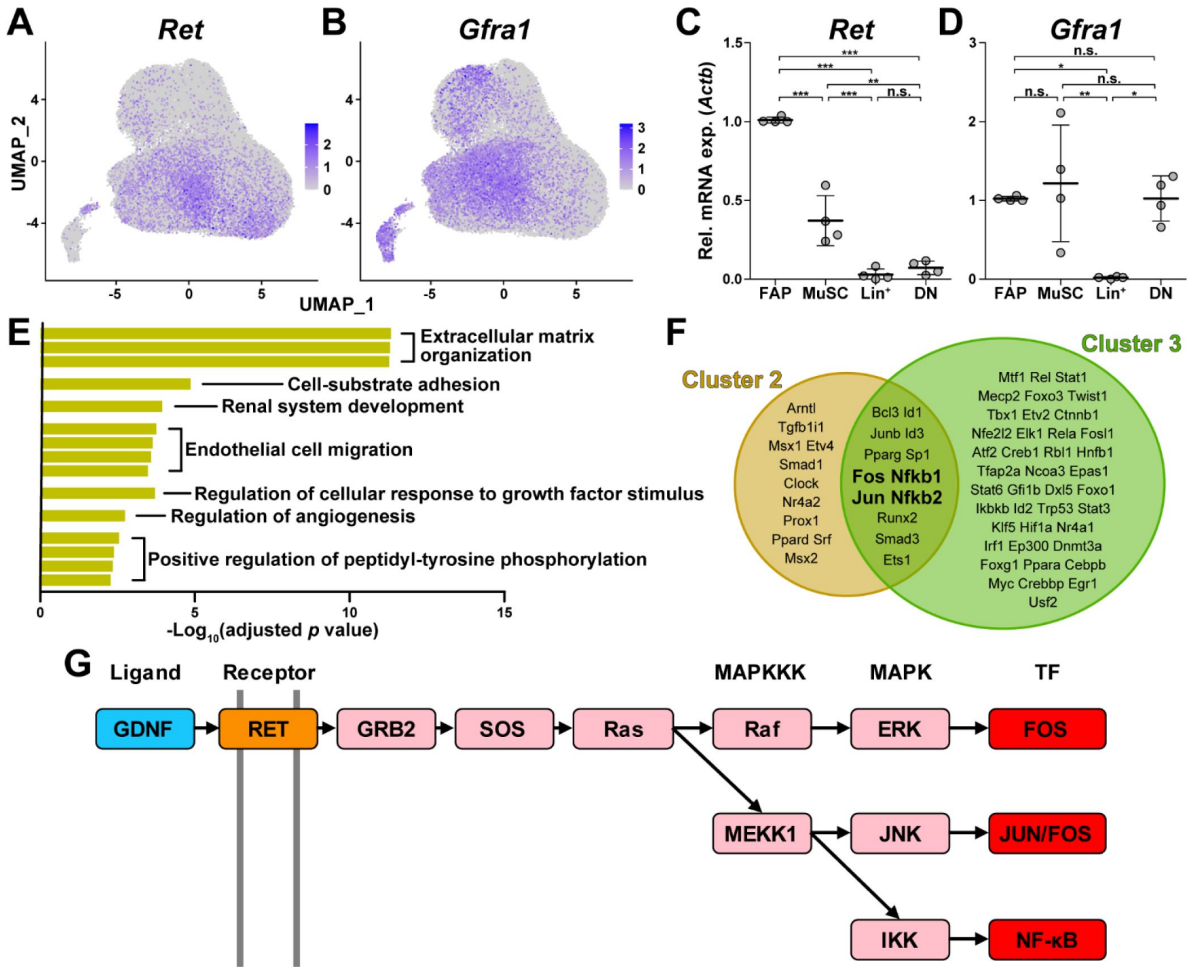

Figure 3.

GDNF signaling pathway in the nerve injury-sensing mechanism by FAPs

(**A**–**B**) UMAP plots showing the expressions of (A) *Ret* and (B) *Gfra1* in the merged scRNA-seq data. (**C**–**D**) RT-qPCR results showing the expressions of (C) *Ret* and (D) *Gfra1* in mononuclear cells isolated from uninjured muscles by FACS. MuSC, muscle stem cells; Lin^+, lineage-positive cells; DN, Vcam1/Sca1 double-negative cells. n = 4; one-way ANOVA with Bonferroni's post hoc test. * $p < 0.05$, ** $p < 0.01$, *** $p < 0.001$, n.s., not significant. (**E**) Shared pathway terms commonly identified from gene set overrepresentation analyses using DEGs specifically upregulated in clusters 1, 2 or 3. (**F**) Venn diagram showing the results from TRRUST analyses using DEGs enriched in clusters 2 and 3. Transcription factors predicted to regulate genes upregulated in each cluster are listed. (**G**) Simplified diagram of the GDNF signaling pathway. Blue: GDNF ligand; orange: GDNF receptor Ret expressed in cluster 1; pink: downstream cascade genes expressed in clusters 1-3; red: transcription factors commonly predicted to regulate upregulated genes in clusters 2 and 3.

lists of DEGs, all of which are known to act downstream of the GDNF/Ret-induced MAPK signaling pathway (Fielder, et al., 2018; Kanehisa, et al., 2023) (**Figure 3F** and **G**, **Figure 3—figure supplement 1C**, **Supplemental tables 1** and **2**). Collectively, robust and specific co-expression of GDNF receptors in cluster 1, together with the prediction of RTK activation and involvement of GDNF signaling pathway downstream TFs in clusters 2 and 3, suggests that GDNF signaling could be the mechanism by which FAPs sense the distant nerve injury, where local Schwann cells act as the GDNF source upon nerve injury.

Bdnf expression in FAPs by both endogenous and exogenous GDNF

Next, to discover how FAPs may contribute to nerve regeneration, we screened the list of genes enriched in clusters 2 and 3 that were predicted to be downstream of the GDNF signaling pathway to identify candidate effector genes. From the TRRUST analysis results, 44 genes were identified to be regulated by either *Fos*, *Jun*, or *NF-κB* (**Figure 4A**, **Supplemental tables 1**–**3**). Since FAPs themselves do not constitute the neural components within skeletal muscle, we reasoned that secreted factors from FAPs would most likely exert beneficial effect on the regenerating nerves. Also, considering the effector gene's potential function in supporting nerve regeneration, we presumed that it regulates neurons or glial cells. Moreover, we anticipated that expression of the effector gene would be limited to the context of nerve injury and regeneration, since the vast majority of FAPs are in a quiescent state in unperturbed adult musclesScott, et al., 2019. Thus, we applied the following criteria to narrow down our candidate gene list: (1) genes that are known to code secreted proteins, (2) genes that are known to regulate neurons or glial cells, and (3) genes that are expressed exclusively in activated FAPs in response to nerve injury (**Figure 4A**, **Supplemental table 3**). Unexpectedly, after filtering out genes that did not fit the three criteria, only *Bdnf* remained in our candidate gene list that could act as the effector secreted by FAPs upon nerve injury to support nerve regeneration (**Figure 4A**). Expression patterns of *Bdnf* in FAPs upon nerve injury showed transient upregulation in SNC-affected FAPs, whereas chronic expression of *Bdnf* was observed in DEN-affected FAPs, showing correlation with its potential requirement during nerve regeneration (**Figure 4C**). The expression of *Bdnf* was mostly limited to cluster 2 (**Figure 4B**), where pathway analysis and TF prediction suggested the involvement of GDNF-Ret-Ras-ERK-Fos signaling cascade in this subset of FAPs (**Figure 3F** and **G**, **Figure 3—figure supplement 1C** and **2A**). Accordingly, we hypothesized that FAPs secrete BDNF in response to GDNF from Schwann cells upon nerve injury, to actively take part in the regeneration process.

To validate our hypothesis *in vivo*, we first examined the expression profiles of *Gdnf* in Schwann cells and *Bdnf* in FAPs at early time points in response to SNC, using $Plp1^{CreER}$; $Rosa^{tdTomato}$ mice to specifically label and hence isolate Schwann cells (Doerflinger, et al., 2003) (**Figure 4D**). Expectedly, we could observe sequential upregulation of *Gdnf* and *Bdnf* from Schwann cells and FAPs, respectively, where *Gdnf* levels peaked at 1 dpi in Schwann cells, followed by a gradual increase of *Bdnf* expression in FAPs, which peaked at 3 dpi (**Figures 4D** and **E**). In addition, to validate the sufficiency of GDNF signaling in inducing *Bdnf* expression in FAPs *in vivo*, we injected recombinant mouse GDNF protein into the TA and the two gastrocnemius (GA) muscles (lateral and medial GA), from which FAPs were FACS-isolated 48 hours post injection to investigate the expression of *Bdnf* (**Figure 4F**). Compared to PBS control, intramuscular injection of GDNF sufficiently induced *Bdnf* expression in FAPs, even in the absence of a nerve injury (**Figure 4F** and **G**). Together, we suggest that FAPs can respond to nerve injury via the GDNF-BDNF axis, since recombinant GDNF protein could sufficiently induce *Bdnf* expression in FAPs without nerve injury, and sequential upregulation of *Gdnf* and *Bdnf* could be observed from Schwann cells and FAPs following nerve injury, respectively.

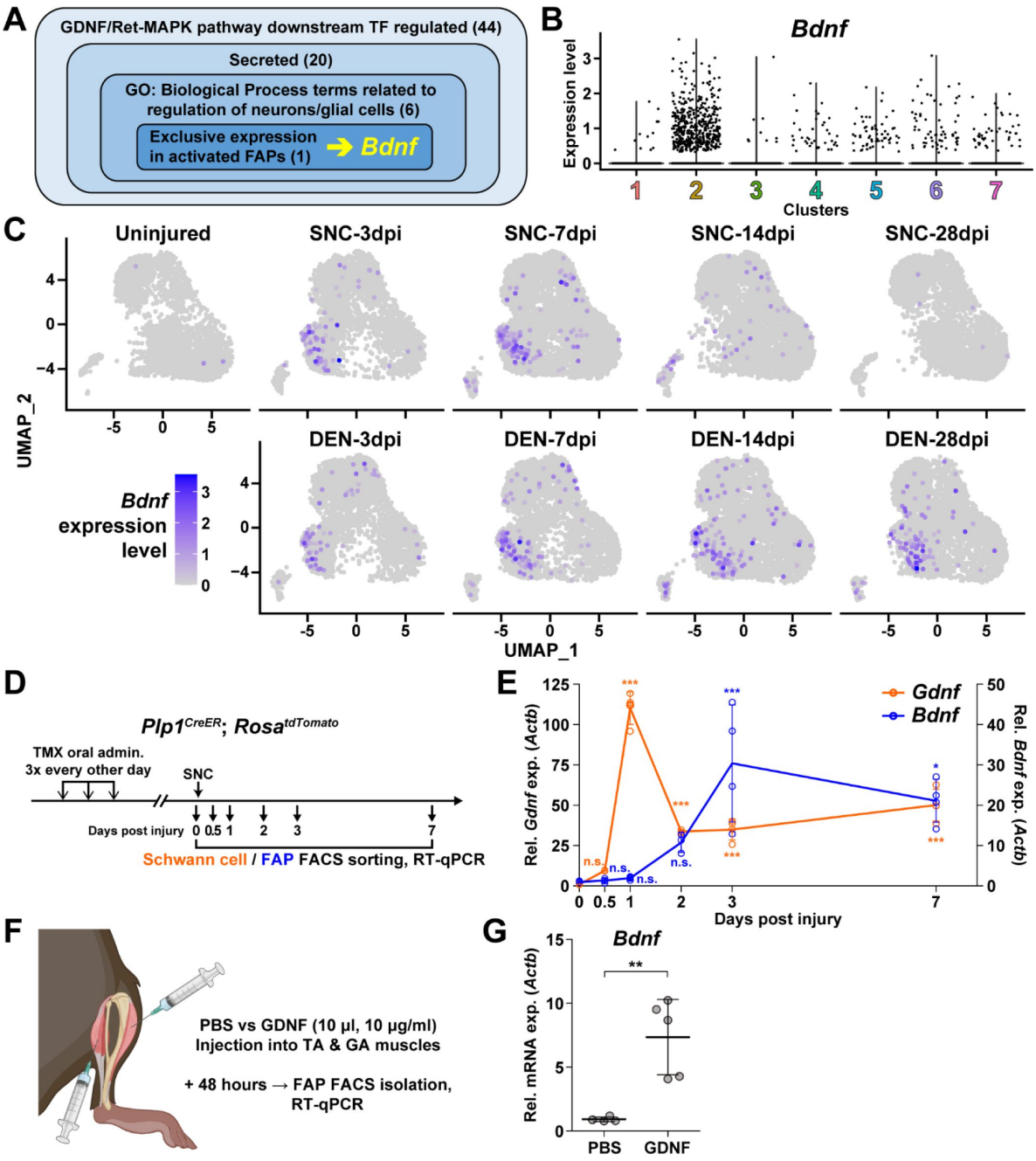

Figure 4.

Bdnf expression in FAPs by both endogenous and exogenous GDNF

(**A**) Scheme for identification of candidate genes expressed in FAPs in response to GDNF that may contribute to nerve regeneration. Number of genes that fit into each criterion is indicated. (**B**) Violin plot displaying the expression levels of *Bdnf* in the seven clusters. (**C**) Expression of *Bdnf* in each scRNA-seq sample shown on UMAP plots. (**D**) Experimental scheme for sampling Schwann cells and FAPs at different time points post SNC for gene expression analyses. (**E**) RT-qPCR results showing the expression levels of *Gdnf* from Schwann cells (orange dot and line, left y-axis) and *Bdnf* from FAPs (blue dot and line, right y-axis) at different time points post SNC displayed on the same plot. n = 4, except for 0 and 2 dpi, where n = 3. One-way ANOVA with Bonferroni's post hoc test. * $p < 0.05$, *** $p < 0.001$, n.s., not significant. (**F**) Experimental scheme for intramuscular injection of either PBS or recombinant mouse GDNF protein, with the time point for FAP isolation post injection indicated. (**G**) RT-qPCR results showing the expression level of *Bdnf* in FAPs 48 hours post intramuscular injection of either PBS (n = 4) or GDNF (n = 5). Unpaired t-test with Welch's correction. ** $p < 0.01$.

Remyelination by FAP-derived BDNF during peripheral nerve regeneration

Although BDNF is known to function in processes such as axon elongation (Oudega and Hagg, 1999; English, et al., 2013), survival of neurons (Ghosh, et al., 1994; Baydyuk and Xu, 2014), and myelination by Schwann cells (Zhang, et al., 2000; Xiao, et al., 2009), the role of BDNF secreted by FAPs in nerve regeneration is unknown. To find out how FAP-derived BDNF can contribute to nerve regeneration, we produced conditional knockout (cKO) mice where *Bdnf* is specifically inactivated in mesenchymal progenitors including FAPs, by crossing $Prrx1^{Cre}$ mice (Logan, et al., 2002; Kim, et al., 2022; Leinroth, et al., 2022; Hann, et al., 2023) with *Bdnf*-floxed ($Bdnf^{fl}$) mice ($Prrx1^{Cre}$; $Bdnf^{fl/fl}$, hereafter cKO) (**Figure 5—figure supplement 1A**). Inactivation of *Bdnf* in FAPs in the cKO mice was confirmed on both genomic DNA and mRNA levels (**Figure 5—figure supplement 1B** and **C**). Though Cre expression in *Prrx1*-expressing cells occur from embryonic day 9.5 (Logan, et al., 2002), no visible phenotypes were observed in the postnatal, juvenile and adult cKO mice compared to littermate controls (hereafter, Ctrl). However, upon SNC in the right hindlimb, cKO mice displayed a delay in nerve regeneration compared to Ctrl, measured by compound muscle action potential (CMAP) amplitude and latency via electromyography (EMG) on the GA muscle (**Figure 5A–5D**, **Figure 5—figure supplement 1D** and **E**). At 4 weeks post injury (wpi), nerve regeneration in both Ctrl and cKO mice showed insufficient recovery in the right, injured GA compared to the left, uninjured GA, where lower amplitude and prolonged latency in CMAP was observed (**Figure 5B–D**). However, at 6 wpi, while CMAP amplitude and latency in the left and right GAs became comparable in Ctrl mice, recovery of such values were stalled at levels comparable to 4 wpi in the cKO mice (**Figure 5B–D**). By 12 wpi, electrophysiological functions of the injured nerves became statistically comparable to that of its contralateral counterpart in the cKO mice, indicating a delayed regeneration in the cKO mice (**Figure 5B–D**).

Generally, decrease in CMAP amplitude and prolonged CMAP latency can be explained by two main causes: axonal loss and defective myelination (Mallik and Weir, 2005; Chung, et al., 2014). Since complete regeneration of the injured nerves on the electrophysiological level could be achieved after a sufficient period of time in the cKO mice (**Figure 5B–D**), we presumed that axonal loss would not have occurred, since it would result in permanent defects by loss of motor units. Instead, we thought that defective myelination could have occurred in the cKO mice, considering the fact that BDNF is already known to promote remyelination during peripheral nerve regeneration (Zhang, et al., 2000; Zheng, et al., 2016), and that defective myelination alone can affect both CMAP amplitude and latency (Mallik and Weir, 2005). Thus, we investigated the effect of conditional *Bdnf* inactivation in FAPs on regenerative myelination by examining the sciatic nerves from Ctrl versus cKO mice at 6 wpi, when the delayed functional recovery of the injured nerves in the cKO mice was prominent (**Figure 5A–D**). Toluidine blue staining of the semi-thin sections of injured sciatic nerves revealed significantly reduced myelin thickness in the cKO mice compared to Ctrl mice (**Figure 5E**). Indeed, higher G-ratio values were calculated from cKO mice compared to Ctrl, confirming the reduced myelination in the regenerating nerves in cKO mice (**Figure 5F**, **Figure 5—figure supplement 1F** and **G**). This decrease in myelin thickness was independent from axon diameter, which were comparable in both Ctrl and cKO mice, implying that no axonal loss or defect had occurred in the cKO mice compared to controls (**Figure 5G**). Taken together, our results revealed the direct involvement of FAP-derived BDNF in the remyelination process during peripheral nerve regeneration, such that inadequate levels of *Bdnf* expression in FAPs caused delayed remyelination and hence delayed nerve regeneration in the cKO mice.

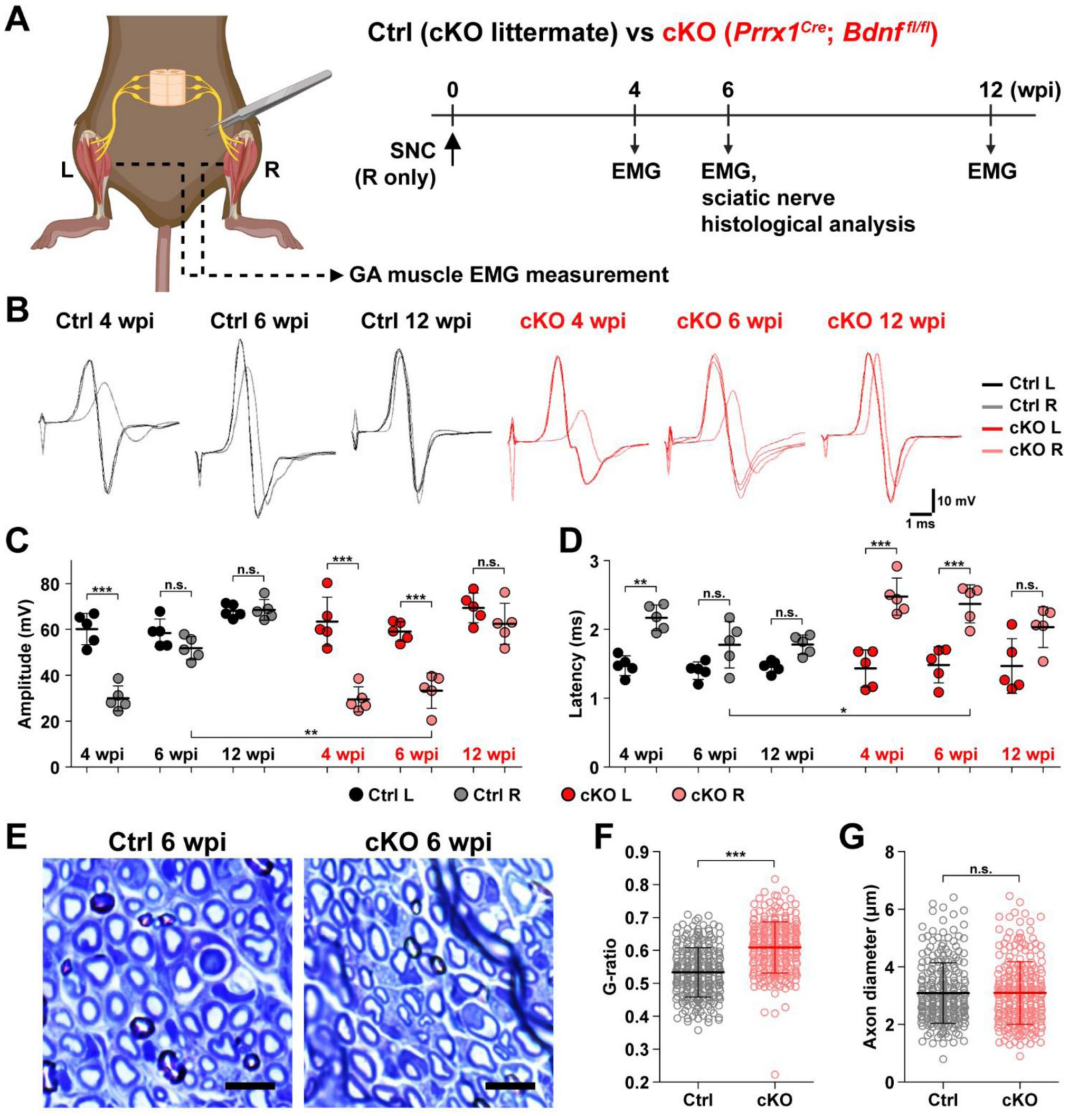

Figure 5.

Remyelination by FAP-derived BDNF during peripheral nerve regeneration

(**A**) Experimental scheme displaying mice used and the time points selected for EMG measurements and sciatic nerve dissection. wpi, weeks post injury. (**B**) Representative EMG measurement results of both injured and uninjured GA muscles from Ctrl or cKO mice at the indicated time points post SNC. (**C**–**D**) Quantified results of EMG measurement showing (C) CMAP amplitude and (D) CMAP latency. n = 5. One-way ANOVA with Bonferroni's post hoc test. * $p < 0.05$, ** $p < 0.01$, *** $p < 0.001$, n.s., not significant. (**E**) Representative images showing toluidine blue-stained, semi-thin cross-sections of sciatic nerves dissected from Ctrl or cKO mice at 6 wpi. Scale bars, 10 μm. (**F**–**G**) Quantification of (F) calculated G-ratio values and (G) axon diameters from analyzing toluidine blue-stained sciatic nerve sections dissected from Ctrl or cKO mice at 6 wpi. 50 axons were randomly selected from each sciatic nerve for quantification. n = 5. Mann-Whitney U test. *** $p < 0.001$, n.s., not significant.

Implication of FAP-derived BDNF in the age-related delay in nerve regeneration

Finally, to seek clinical relevance of *Bdnf* expression in FAPs during nerve regeneration, we compared the expression levels of *Bdnf* in adult (5-6 months) versus aged (24 months) mice in FAPs post SNC. At 7 dpi, *Bdnf* expression was significantly reduced in the aged mice compared to adult mice (**Figure 6A** and **B**). Such a difference could be one of the factors that lead to the delayed or failed regeneration of injured nerves in the elderly compared to healthy, young adults, suggesting the clinical role of FAPs in a timely, successful peripheral nerve regeneration process.

Discussion

Traumatic injury to the peripheral nerve has severe consequences, including lifelong paralysis of the injured limb that can compromise the quality of life significantly (Grinsell and Keating, 2014). Thus, understanding the regeneration process of the peripheral nerves is fundamental for treating the potentially devastating injury. Previously, several cellular components in and outside the injured nerve were discovered to actively participate in the regeneration process, including the injured neurons (Hanz, et al., 2003), glial cells (Arthur-Farraj, et al., 2012), immune cells (Mueller, et al., 2001; Kalinski, et al., 2020), and nerve-resident mesenchymal cells (Parrinello, et al., 2010; Toma, et al., 2020), via diverse mechanisms so that the nerve can regain its function (Scheib and Hoke, 2013). In this study, we investigated the response mechanism of muscle-resident FAPs to both acute and chronic peripheral nerve injury via scRNA-seq, and revealed that this population of cells can also actively take part in the nerve regeneration process. Here, we discovered that muscle-resident FAPs can recognize the distant nerve injury by sensing GDNF secreted by Schwann cells. Though GDNF secretion by Schwann cells in response to nerve injury had previously been recognized (Hammarberg, et al., 1996; Hoke, et al., 2002; Arthur-Farraj, et al., 2012; Xu, et al., 2013; Proietti, et al., 2021), we identified FAPs as a major target cell population of GDNF within skeletal muscle, based on the enriched expression of GDNF receptors. In depth, exploiting the technical advantage of scRNA-seq, we suggested that a subset of FAPs, named cluster 1 in this study, can sense the local GDNF by expressing GDNF receptors *Ret* and *Gfra1*, and that upon GDNF sensing, cluster 1 FAPs turn into clusters 2 and 3 to contribute to the nerve regeneration process. Specifically, we discovered that FAPs, especially the *F2rl1*-expressing cluster 2, express *Bdnf* in response to nerve injury and/or GDNF, which in turn was shown to promote the remyelination process by Schwann cells during nerve regeneration, using our cKO mouse model (**Figure 6C**). Since epineurial and perineurial, but not endoneurial mesenchymal cells share their origins with the muscle-resident FAPs and therefore are *Prrx1*-positive (Joseph, et al., 2004; Carr, et al., 2019), the possibility that the delayed remyelination observed in our cKO mice could be due to the combined effect of *Bdnf* depletion in both muscle- and nerve-resident mesenchymal cells cannot be eliminated. To resolve such issue, further investigations using muscle-resident FAP-specific Cre mouse lines is required, but such line is currently unavailable as no such specific marker has been found. Nevertheless, our findings show that muscle-resident FAP-derived BDNF is indeed important for nerve regeneration, since intramuscular injection of recombinant BDNF can sufficiently accelerate the nerve regeneration process (Zheng, et al., 2016). Conversely, intramuscular injection of BDNF-neutralizing antibodies can sufficiently delay nerve regeneration (Zheng, et al., 2016). Thus, endogenous supply of intramuscular BDNF by the muscle-resident FAPs in our Ctrl mice would likely have supported remyelination by Schwann cells, while the lack of such BDNF supply by FAPs in our cKO mice would have resulted in delayed remyelination. Also, we found that while muscle-resident FAPs robustly express both GDNF receptor genes, neither epineurial nor perineurial mesenchymal cells express significant levels of *Ret* and *Gfra1* (**Supplemental figure 1**), implying that the GDNF-BDNF axis found in this study could be valid uniquely in muscle-resident FAPs. Collectively, we suggest that muscle-resident mesenchymal progenitors can directly contribute to nerve

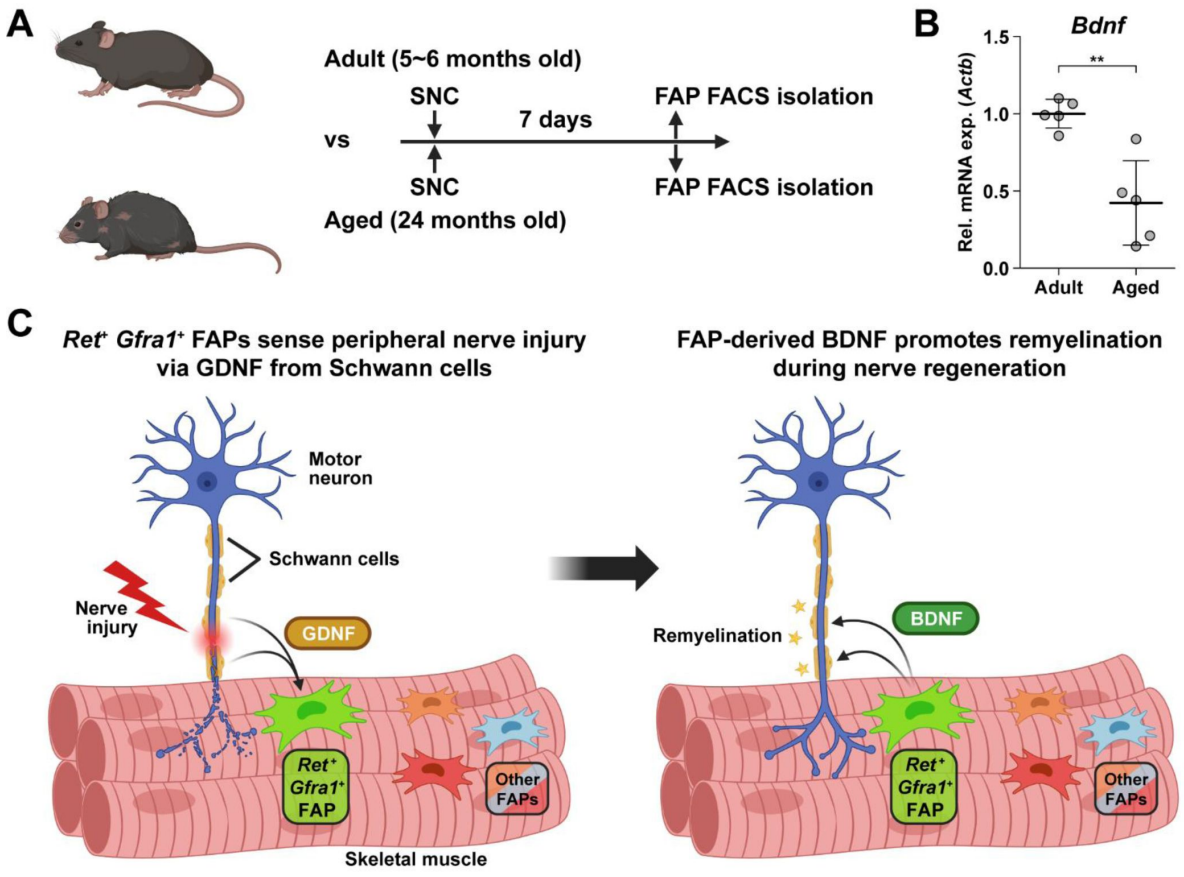

Figure 6.

Implication of FAP-derived BDNF in the age-related delay in nerve regeneration

(**A**) Experimental scheme indicating ages of mice used and the time point for FAP isolation to compare the expression level of *Bdnf* post SNC. (**B**) RT-qPCR results showing the expression level of *Bdnf* in FAPs isolated from either adult (5-6 months) or aged (24 months) mice at 7 dpi. n = 5. Unpaired t-test. ** $p < 0.01$. (**C**) Graphical summary of this study.

regeneration via the GDNF-BDNF axis (**Figure 6C**), of which was previously unidentified; we suggest that in future studies regarding peripheral nerve regeneration, active participation of this intramuscular mesenchymal population should be taken into consideration. In that process, our scRNA-seq data may provide valuable insights, which may lead to additional discoveries on FAP's contributions to nerve regeneration by other mechanisms, and/or provide clues on the cell-to-cell communications of FAPs with other cell types that may lead to facilitation of the regeneration process.

Here, we have primarily investigated the roles of *Ret*-expressing and *F2rl1*-expressing FAPs in sensing and responding to nerve injury, respectively. However, possibilities that other subpopulations can exert distinct beneficial effects on nerve regeneration remain largely unexplored. For example, although identified as a nerve injury-relevant subpopulation in this study, specific contributions of the *Alkal2*-expressing cluster 3 FAPs to nerve regeneration are yet to be discovered. Identification of effector genes such as *Bdnf* from this subpopulation may lead to the discovery of an additional mechanism by which FAPs can contribute to nerve regeneration. Although other subpopulations (clusters 4-7) did not exhibit dramatic fluctuations in population percentage, some of the genes expressed specifically in those subpopulations showed patterns that followed the regeneration process (**Supplemental figure 2**). Such gene expression patterns suggest subpopulation-specific functions even in the less dynamic subpopulations within FAPs in peripheral nerve regeneration, and require further investigations to reveal their possible contributions.

The role of BDNF in peripheral nerve regeneration has been identified previously, where it was found to promote both intrinsic axonal regeneration in neurons as well as remyelination by Schwann cells (Zhang, et al., 2000; Zheng, et al., 2016). In such circumstances, various cellular sources of BDNF have been identified. Bone marrow transplantation of wild-type cells into *Bdnf* heterozygotic knockout mice revealed the involvement of bone marrow-derived cells in expressing *Bdnf* that can promote nerve regeneration in the sciatic nerve (Takemura, et al., 2012). Schwann cells themselves are cellular sources of BDNF during nerve regeneration (Wilhelm, et al., 2012). In this study, we showed that BDNF from FAPs can also promote myelination of the regenerating axons post injury, suggesting FAPs as an additional cellular source of BDNF in peripheral nerve regeneration. The existence of cellular sources of BDNF other than FAPs such as Schwann cells would provide an explanation for the delayed, but not failed, remyelination in our *Bdnf* cKO mice, where complete regeneration had occurred after a sufficient amount of time, despite the lack of *Bdnf* expression in FAPs. Still, ablation of *Bdnf* in FAPs displayed significant delays in the remyelination process during nerve regeneration, suggesting their requirement in the timely regeneration process of injured nerves. Meanwhile, scRNA-seq data of all mononuclear cells from denervated muscles (Nicoletti, et al., 2023) suggested expression of *Bdnf* in tenocytes and pericytes in addition to Schwann cells and FAPs (**Supplemental figure 3A** and **B**). Although this may imply the involvement of those cellular components in providing BDNF for nerve regeneration, expression of *Bdnf* in such cells were not altered as significantly in response to nerve injury as in FAPs or Schwann cells (**Supplemental figure 3C**). Moreover, while *Ret*-expressing FAPs and Schwann cells are known to be in proximity to the NMJ or relevant nerve regeneration sites (Leinroth, et al., 2022), such locational enrichment of tenocytes and pericytes have not been reported so far. Thus, it is likely that FAPs, together with Schwann cells, are the main sources of BDNF within skeletal muscle that can act in the remyelination process during peripheral nerve regeneration.

Aging is one of the well-known factors that can slow down the nerve regeneration process (Verdú, et al., 2008; Maita, et al., 2023). Since multiple cell types are known to participate in this process (Scheib and Hoke, 2013), determination of the cell types that can cause age-related delays in nerve regeneration is important for the development of therapeutic approaches targeting the relevant cell types. Of note, previous research emphasized the importance of niche factors, rather than the intrinsic regenerative capacity of the injured neurons, in the age-related

decline in nerve regeneration (Painter, et al., 2014). Specifically, inability of Schwann cells to adopt repair cell phenotypes has been pointed out as one of the age-related changes (Painter, et al., 2014; Wagstaff, et al., 2021). In addition, age-related changes in immune cells, especially macrophages, were suggested as causal factors that delay nerve regeneration (Buttner, et al., 2018). In particular, chronic inflammatory phenotypes were shown to interfere with the remyelination process by Schwann cells (Buttner, et al., 2018), and failed macrophage infiltration in the early stages of regeneration resulted in defective Wallerian degeneration and myelin debris clearing (Scheib and Hoke, 2016). In addition to the involvement of Schwann cells and immune cells, we have identified muscle-resident FAPs as an additional cellular component that can contribute to nerve regeneration, by promoting remyelination via BDNF secretion. Surprisingly, expression of *Bdnf* by FAPs was significantly reduced in aged mice compared to adult mice, suggesting the clinical relevance of FAP's involvement in the age-related delay in peripheral nerve regeneration. We believe that further studies on age-related changes in FAPs may provide valuable clues to understanding clinical observations from aged individuals, which can lead to development of additional therapeutic strategies that include FAPs as target cells in treating both young and aged nerve injury patients.

Materials and Methods

Animals

C57BL/6J (RRID:IMSR_JAX:000664), $Prrx1^{Cre}$ (RRID:IMSR_JAX:005584), $Bdnf^{fl}$ (RRID:IMSR_JAX:004339), $Plp1^{CreER}$ (RRID:IMSR_JAX:005975) and $Rosa^{tdTomato}$ (RRID:IMSR_JAX:007914) mice were all obtained from The Jackson Laboratory. To generate $Prrx^{Cre}$; $Bdnf^{fl/fl}$mice, $Prrx^{Cre/+}$; $Bdnf^{fl/+}$ males and $Bdnf^{fl/fl}$females were crossed to avoid germline recombination in the female reproductive cells, and littermates were used as controls. To generate $Plp1^{CreER}$; $Rosa^{tdTomato}$ mice, $Plp1^{CreER/+}$ mice were crossed with $Rosa^{tdTomato/+}$ mice, and the line was kept by breeding $Plp1^{CreER/+}$; $Rosa^{tdTomato/tdTomato}$ males and females. Only mice that had the $Plp1^{CreER}$ allele was used. Primers used for genotyping are listed in **Supplemental table 4**. All mice were bred on the B6 background, except for the $Prrx^{Cre}$; $Bdnf^{fl/fl}$ mice and littermates that were kept in the mixed B6, 129S4 and BALB/c background. All mice were housed in a specific-pathogen-free (SPF) animal facility, with 12-h light/12-h dark cycle at room temperature (RT, 22℃) and 40~60% humidity, and were fed with normal chow diet and water ad libitum. Tamoxifen administration, sciatic nerve crush injury, denervation and intramuscular GDNF injections were all given to 3 to 4-month-old adult mice. When comparing aged mice versus adult mice, 24-month-old and 5 to 6-month-old mice were used, respectively. In all cases except for $Plp1^{CreER}$; $Rosa^{tdTomato}$ mice, male mice were used for the experiments. No sex-specific differences were observed in experiments using $Plp1^{CreER}$; $Rosa^{tdTomato}$ mice. All experimental procedures were approved by the Institutional Animal Care and Use Committtee at Seoul National University and were carried out according to the guidelines provided.

Tamoxifen administration

To label Schwann cells, 3-month-old $Plp1^{CreER}$; $Rosa^{tdTomato}$ mice were administered orally with tamoxifen (20 mg/ml in corn oil, 160 mg/kg body weight; Sigma-Aldrich) 3 times every other day.

Sciatic nerve injury

Mice were deeply anesthesized via intraperitoneal injection of Avertin (32 mg/ml, ~800 mg/kg; Sigma-Aldrich), and the incision site on the posterior side of the right hindlimb was shaved and depilated using surgical clippers and hair removal cream. After cleansing the incision site with 70% ethanol, incision was made on the skin with surgical scissors and the biceps femoris muscle was punctured open with fine-tip forceps to expose the sciatic nerve. For sciatic nerve crush injury, the exposed nerve was crushed with fine forceps for 30 seconds at the site just proximal to

where the tibial, peroneal and sural nerves branched out from the sciatic nerve. For denervation, ~5 mm of the sciatic nerve proximal from the crush injury site was cut and removed. The punctured biceps femoris muscle and skin were then sutured, and the incision site was sterilized with povidion-iodine.

Intramuscular injection of GDNF

Tibialis anterior muscle and the two gastrocnemius muscles (GA, lateral and medial) were each injected with 10 µl of either PBS or recombinant mouse GDNF (10 µg/ml, Sigma-Aldrich) using 31-gauge insulin syringes without damaging any innervating nerves. The injected muscles were then dissected 48 hours post injection for isolation of FAPs and further analysis.

Isolation of FAPs, Schwann cells and others

Isolation of muscle-resident FAPs, Schwann cells and others was performed according to a previously reported protocol (Liu, et al., 2015) with minor modifications. Muscles indicated in each experiment were dissected, finely chopped with surgical scissors and washed with 10% horse serum (Gibco), DMEM (HyClone) for further dissociation. Enzymatic dissociation was carried out in 10% horse serum, DMEM containing collagenase II (800 U/ml, Worthington Biochemical) and dispase II (1.1 U/ml, Gibco) for 40 minutes at 37℃ with mild agitation, and mechanical dissociation was performed by tituration of the dissociated solution with a 20-gauge needle ten times. After filtering the solution through a 40 µm strainer, dissociated mononuclear single cells were stained with the following antibodies: APC anti-mouse CD31, APC anti-mouse CD45, PE anti-mouse TER-119, Biotin anti-mouse CD106 (Vcam1) (Biolegend) and FITC anti-mouse Ly-6A/E (Sca1) (BD Pharmingen); 7-aminoactinomycin D (7-AAD, Sigma-Aldrich) was added to stain dead cells. Gating strategies used for the isolation of each cell type were as follows: FAPs, 7-AAD$^-$Ter119$^-$CD31$^-$CD45$^-$Vcam1$^-$Sca1$^+$; MuSCs, 7-AAD$^-$Ter119$^-$CD31$^-$CD45$^-$Vcam1$^+$Sca1$^-$; lineage-positive cells, 7-AAD$^-$Ter119$^-$CD31$^+$ or 7-AAD$^-$Ter119$^-$CD45$^+$; double-negative cells, 7-AAD$^-$Ter119$^-$CD31$^-$CD45$^-$Vcam1$^-$Sca1$^-$. For Schwann cells, 7-AAD$^-$tdTomato$^+$ cells were sorted from tamoxifen-administered *Plp1*^{CreER}; *Rosa*^{tdTomato} mice.

scRNA-seq library construction and sequencing

FAPs were isolated from sciatic nerve crush injury-affected or denervated muscles on days 3, 7, 14 and 28 post injury using wild type B6 mice, so that a total of nine samples, including uninjured control, were collected for library generation. For each sample, isolated FAPs were pooled from two mice. Chromium Next GEM Single Cell 3′Kit v3.1 (10x Genomics) was used according to the manufacturer's instructions for the nine collected FAP samples, and target cell number for recovery was set to 5,000 in each sample. Sequencing of the libraries was carried out using HiSeq X Ten (Illumina).

Computational analysis of scRNA-seq data

Sequenced reads were aligned to the mouse reference genome mm10 using CellRanger v3.1.0 (10x Genomics), and aligned reads were transformed into gene-cell count matrices using velocyto v0.17 (La Manno, et al., 2018) to obtain count matrices for both spliced and unspliced mRNAs. Output loom files were then loaded with R package SeuratWrappers v0.3.1, and were preprocessed and analyzed using R package Seurat v4.3.0 (Hao, et al., 2021) for downstream analysis. The preprocessing steps for quality control included doublet filtering, live cell filtering and removal of non-FAPs as previously described (Kim, et al., 2022). All nine sample data were merged and normalized for dimensionality reduction, where top 8 principal components from the principal component analysis using 5,000 variable genes were selected for 2-dimensional UMAP embedding and visualization. Unsupervised clustering of cells was achieved through FindNeighbors and FindClusters functions in Seurat R package. To identify DEGs in the pairwise comparisons of scRNA-seq samples, the FindMarkers function in Seurat R package was used with the following parameters: fold change >= 2, pseudocount.use = 0.01, min.pct = 0.01, adjusted p value < 0.05. For

identification of DEGs in each cluster, FindAllMarkers function was used with the parameters: fold change >= 1.5, pseudocount.use = 0.01, min.pct = 0.02, adjusted p value < 0.05. For hierarchical clustering, R package pheatmap v1.0.12 was used. For RNA velocity analysis, R package velocyto.R v0.6 was used following the instructions provided by the developer (La Manno, et al., 2018). For the prediction of upstream regulatory transcription factors using lists of DEGs enriched in the selected FAP clusters, the web-based tool TRRUST v2 (Han, et al., 2018) was used. For color mapping of the MAPK signaling pathway, online version of the KEGG Mapper – Color (Kanehisa, et al., 2023) was used.

Gene set overrepresentation analysis

To identify pathways enriched in the lists of DEGs, web-based version of g:Profiler (Kolberg, et al., 2023) was used with the following parameters: organism – Mus musculus; ordered query – YES; data sources – GO biological process without electronic GO annotations, Reactome, and WikiPathways; advanced options were set to default. Visualization of the results were done as previously described (Reimand, et al., 2019), using the Cytoscape v3.10.1 (Shannon, et al., 2003) application with tools EnrichmentMap v3.3.6 (Merico, et al., 2010) and AutoAnnotate v1.4.1 (Kucera, et al., 2016).

RNA extraction and qRT-PCR

Total RNA extraction and reverse transcription was carried out for isolated FAPs, Schwann cells, MuSCs and others using TRIzol™ reagent (Invitrogen) and ReverTra Ace™ qPCR RT Master Mix (Toyobo) reagents respectively, following the manufacturer's instructions. qPCR was performed using ORA™ SEE qPCR Green ROX L Mix (HighQu) reagent, with gene-specific primers listed in **Supplemental table 4**. Quantitative analysis of mRNA levels were done using the $2^{-\Delta\Delta Ct}$ method with β-actin (*Actb*) as the housekeeping gene for normalization.

Electromyography and CMAP measurement

Intraperitoneal injection of Avertin (32 mg/ml, ~800 mg/kg) for anesthetization of mice was carried out prior to CMAP measurement. Stimulation of the sciatic nerve was achieved by placing stimulating electrodes subcutaneously on either side of the sciatic notch and applying supramaximal stimuli (~70 mA) at a rate of 1 pulse per second with the duration of 0.1 ms, using Isolated Pulse Stimulator Model 2100 (A-M Systems). Recording electrode was placed carefully on the GA muscle subdermally without puncturing the muscle, with the reference electrode placed near the Achilles tendon and ground electrode placed on the tail for data recording using Data Recorder IX-RA-834 (iWorx). CMAP amplitude was determined by the absolute difference between potentials of positive and negative peaks, and CMAP latency was determined by the delay from stimulus peak to the beginning of response peak. Three individual measurements were taken from each animal's GA muscle, and average values were used as representatives for statistical analysis.

Toluidine blue staining of sciatic nerves

Sciatic nerve distal to the injury site was dissected at 6 weeks post injury for analysis. The dissected nerves were fixed in 4% paraformaldehyde dissolved in Sorensen's phosphate buffer (0.1M, pH 7.2) at 4°C overnight, followed by procedures described previously (Kim, et al., 2022) with minor modifications for semi-thin sectioning. Briefly, fixed samples were washed with 0.1M sodium cacodylate buffer (pH 7.2), post-fixed with 1% osmium tetroxide in 0.1M sodium cacodylate buffer (pH 7.2) for 1 hour at RT, washed with distilled water (DW) and stained with 0.5% uranyl acetate at 4°C overnight. Stained samples were then washed with DW and dehydrated using serial ethanol and propylene oxide. Samples were then embedded in Spurr's resin (Electron Microscopy Sciences), and semi-thin sections (500 nm) were prepared with a diamond knife on an ultramictorome EM UC7 (Leica). The sections were dried down on glass slides for staining and light

microscopy. Toluidine blue staining were done using 1% toluidine blue solution containing 1% sodium borate on a slide warmer (70°C), and images were obtained with the light microscope EVOS FL Auto 2 (Thermo Fisher Scientific) for analysis.

G-ratio quantification

Semi-automated quantification of naked and myelinated axon diameters were carried out using an ImageJ plugin for g-ratio quantification (Goebbels, et al., 2010), where axon diameters and G-ratios were quantified and calculated, respectively. G-ratios were calculated as [naked axon diameter]/[myelinated axon diameter].

Quantification and statistical analysis

All statistical analyses were performed using Prism v5.01 (GraphPad) and R v4.2.1. Continuous variables were tested for normal distribution with Shapiro-Wilk test, and F-test was used to check for equal variance. For comparison of significant differences in multiple groups, one-way analysis of variance(ANOVA) followed by Bonferroni's pairwise post hoc test was applied. For comparison of two groups, unpaired t-test was used for data with normal distribution and equal variance; Welch's t-test was used for data with normal distribution and unequal variance; and Mann-Whitney U test was used for non-normally distributed data. ANCOVA was applied to test for differences between slopes of linear regression lines. Two-way ANOVA was applied to compare two groups with two variables. For comparison of gene expression levels between scRNA-seq data, Wilcoxon rank sum test was applied as a default in functions FindAllMarkers and FindMarkers within the R package Seurat v4.3.0. For RT-qPCR, the average of triplicate technical values were used for each biological replicate. All error bars represent mean ± SD. P value of less than 0.05 was considered statistically significant at the 95% confidence level. The number of technical and biological replicates and statistical analysis used in each experiment are indicated in the figure legends.

Data availability

Single-cell RNA-sequencing data produced in this study have been deposited at GEO under accession number GSE250436 and are publicly available as of the date of publication.

Acknowledgements

We thank Dr. Jong-Eun Park for his helpful comments on the analysis of our scRNA-seq data. *Prrx1*^{Cre} mice, *Bdnf*^{fl}mice, and *Plp1*^{CreER} mice were obtained via Korea Mouse Phenotyping Center, deposited by Dr. Rho Hyun Seong, Dr. Yun-Hee Lee, and Dr. Myunghwan Choi, respectively. Also, we would like to acknowledge technical support from Center for Research Facilities, Biological Sciences Department, Seoul National University (SNU) and SNU National Instrumentation Center for Environmental Management. Library construction and sequencing of the scRNA-seq data was performed by Macrogen Inc.. Experimental schemes and graphical summary in this paper were created using BioRender. This work was supported by grants from the National Research Foundation of Korea (NRF-2020R1A5A1018081, NRF-2022R1A2C3007621) funded by the Korean government (MSIT).

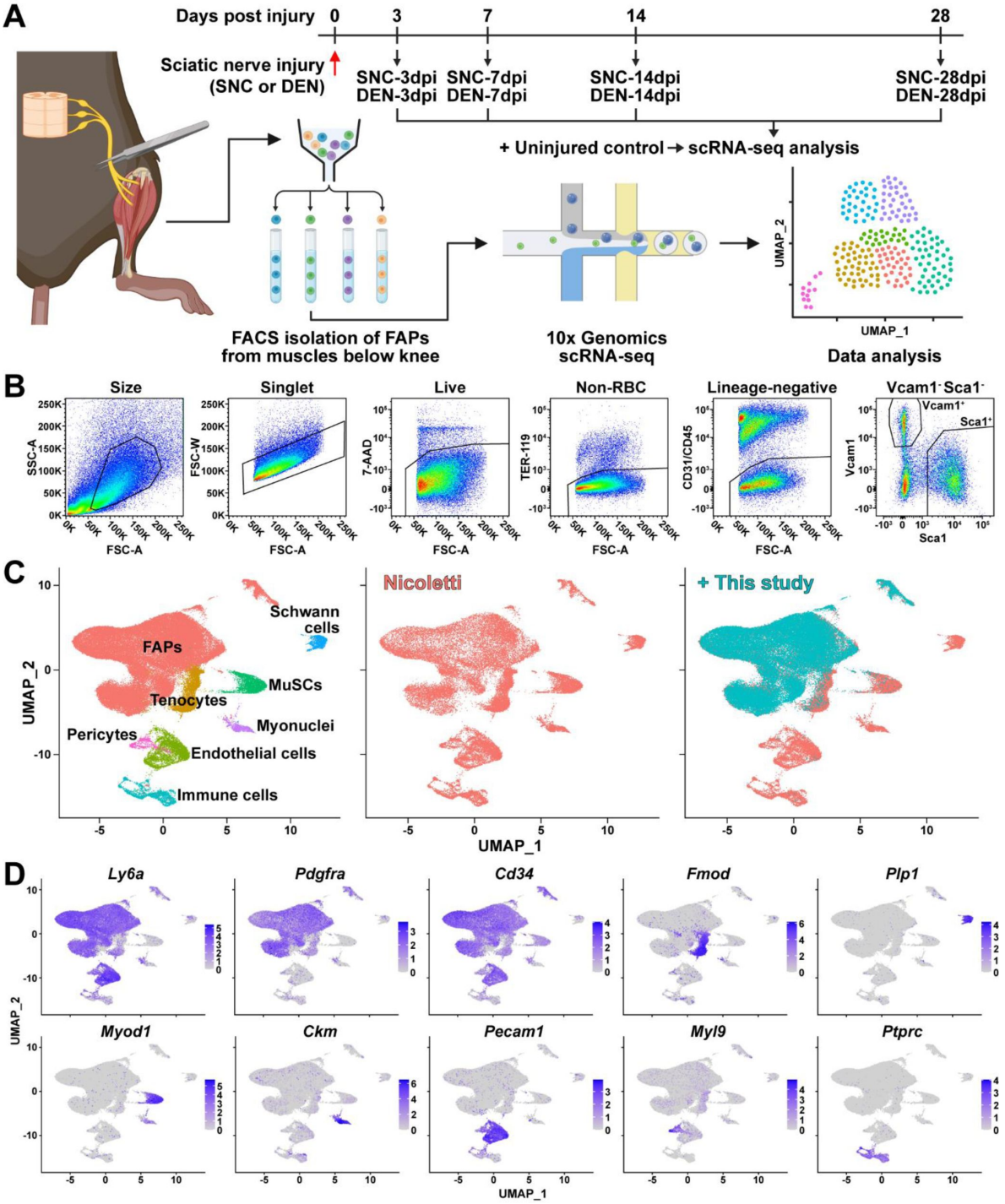

Figure 1—figure supplement 1.

Establishment and validation of nerve injury-affected FAPs' scRNA-seq data

(**A**) Experimental scheme depicting the procedures for sample collection and scRNA-seq. The types of nerve injuries and time points for FAP isolation for each sample are specified. (**B**) Gating strategies used for FACS isolation of FAPs. (**C**) Integration of scRNA-seq data obtained in this study and data from Nicoletti et al. (2023) visualized on UMAP plots. Left: integrated data labeled with cell types; middle: cells from Nicoletti et al. (2023) only; right: data from this study overlaid on top of data from Nicoletti et al. (2023). (**D**) Expressions of marker genes that distinguish cell types within skeletal muscle in the integrated scRNA-seq data visualized on UMAP plots.

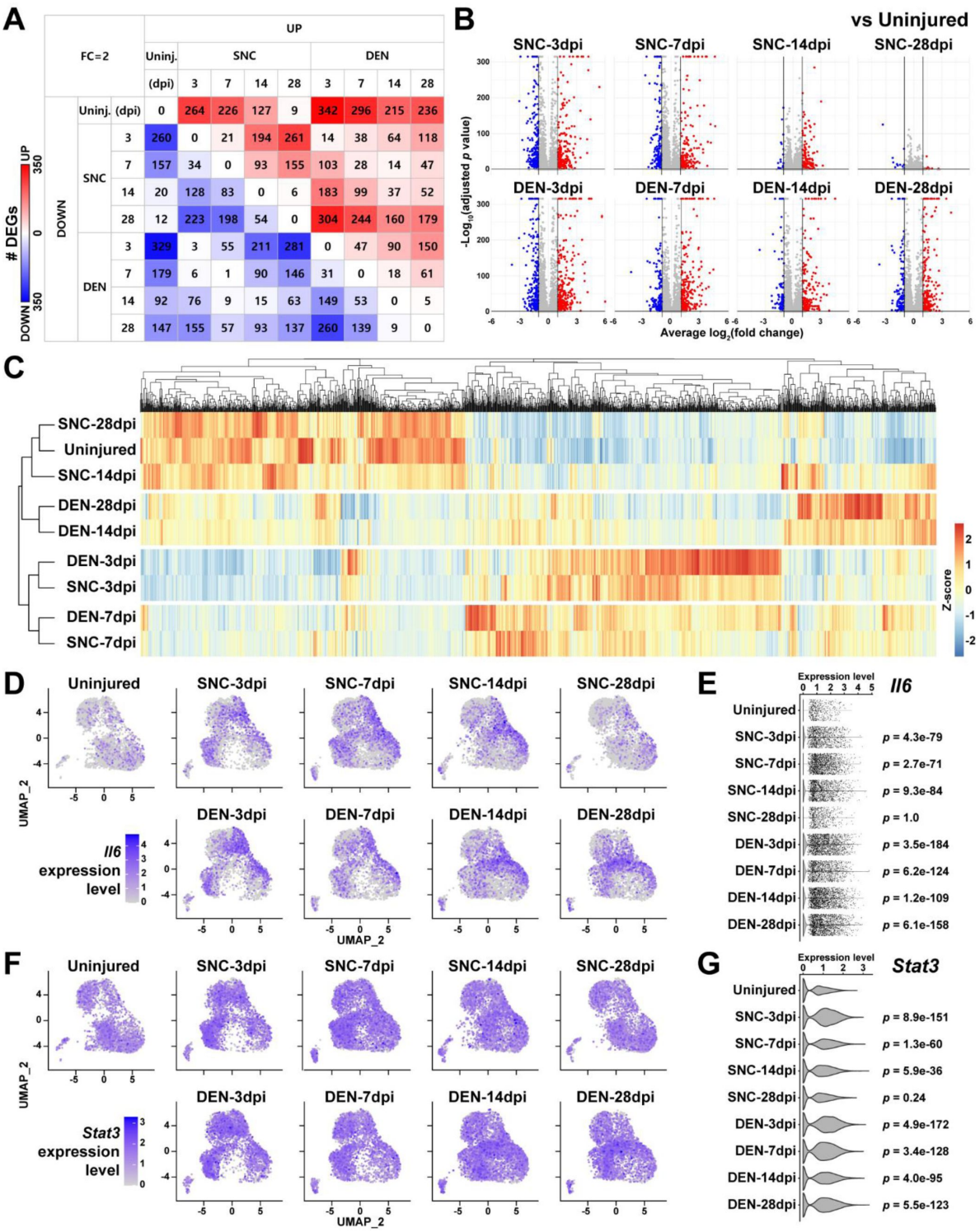

Figure 1—figure supplement 2.

DEG analyses reveal similarities and differences between FAPs affected by SNC or DEN at different time points

(**A**) Number of DEGs identified from pairwise comparisons of all nine scRNA-seq samples visualized as a heatmap. (**B**) DEGs identified from comparing nerve injury-affected FAPs versus uninjured control shown on volcano plots. (**C**) Hierarchical clustering of the nine scRNA-seq samples using DEGs identified in (A) displayed as a heatmap. (**D** and **F**) UMAP plots showing the expressions of (D) *Il6* and (F) *Stat3*. (**E** and **G**) Violin plots showing the expressions of (E) *Il6* and (G) *Stat3*, with p values calculated from comparing each sample to uninjured control. Wilcoxon rank sum test.

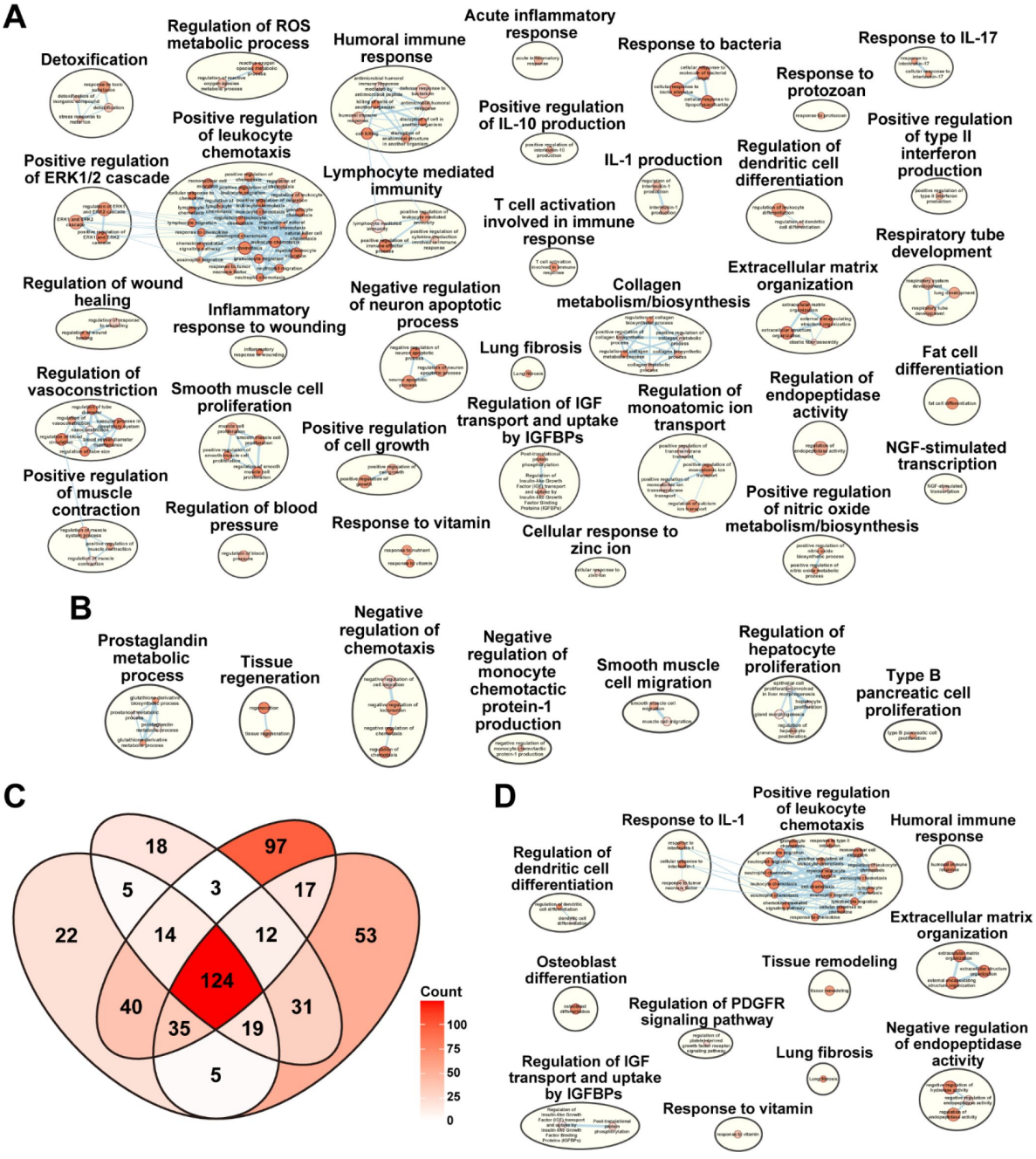

Figure 1—figure supplement 3.

Gene set overrepresentation analyses using DEGs from pairwise comparisons of the nine scRNA-seq samples

(**A–B**) Results from g:Profiler showing pathways enriched using DEGs upregulated in (A) DEN-28dpi versus SNC-28dpi and (B) vice versa. (**C**) Venn diagram showing the number of overlapping genes identified as DEGs by comparing each indicated sample to uninjured control. (**D**) Results from g:Profiler showing pathways enriched using DEGs shared in all four samples compared to uninjured control, as shown in (C).

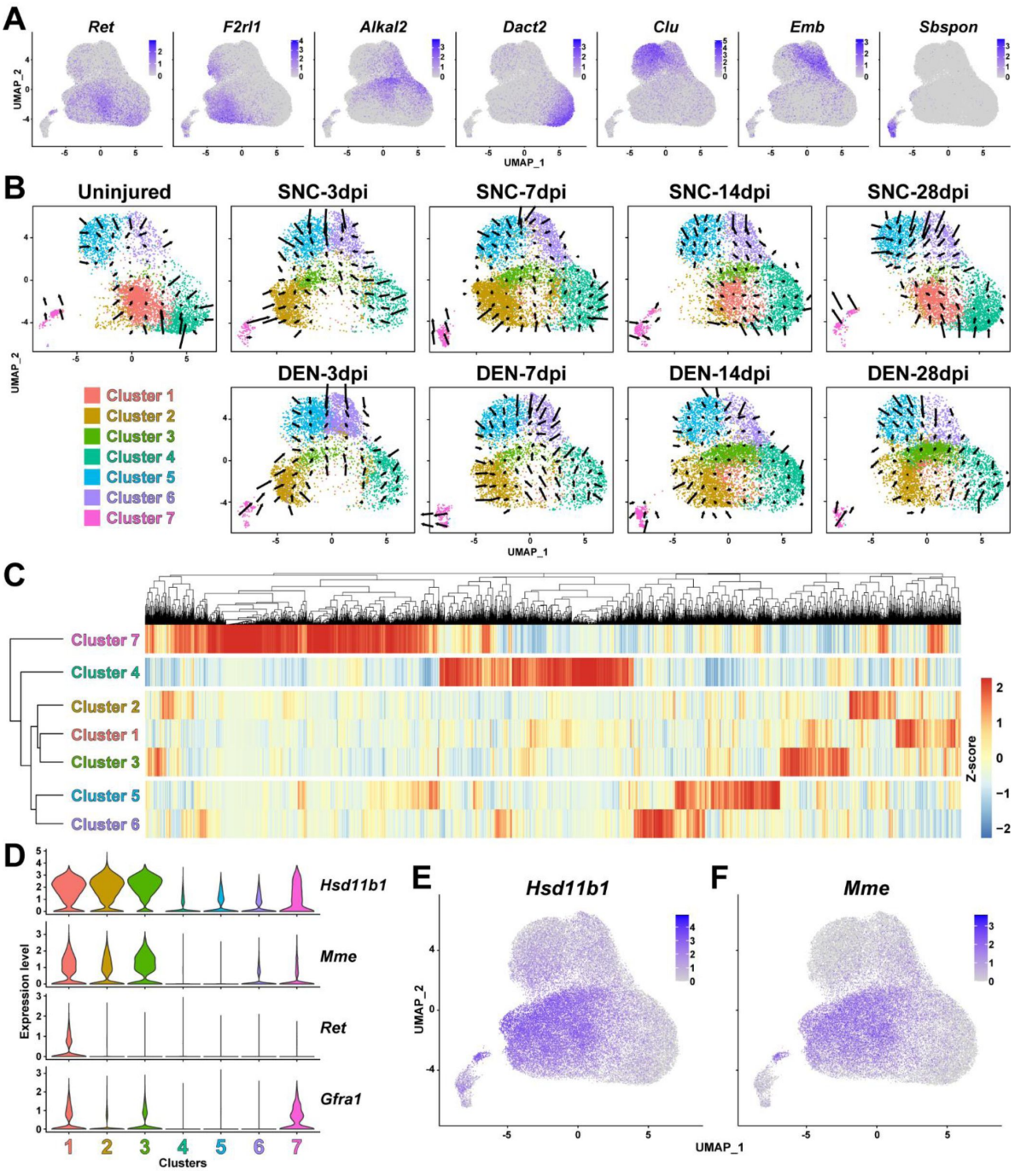

Figure 2—figure supplement 1.

Identification of FAP clusters that respond to nerve injury

(**A**) UMAP plots showing expressions of cluster-specific marker genes identified in this study. (**B**) Results from RNA velocity analysis visualized on UMAP plots. Arrows indicate the predicted direction of cellular movement in the near future on the UMAP plots. (**C**) Hierarchical clustering of the seven FAP clusters displayed with a heatmap. (**D**) Violin plots showing the expressions of marker genes previously reported by Leinroth et al. (2022) in the seven clusters identified in this study. (**E–F**) Expressions of (E) *Hsd11b1* and (F) *Mme* shown on UMAP plots.

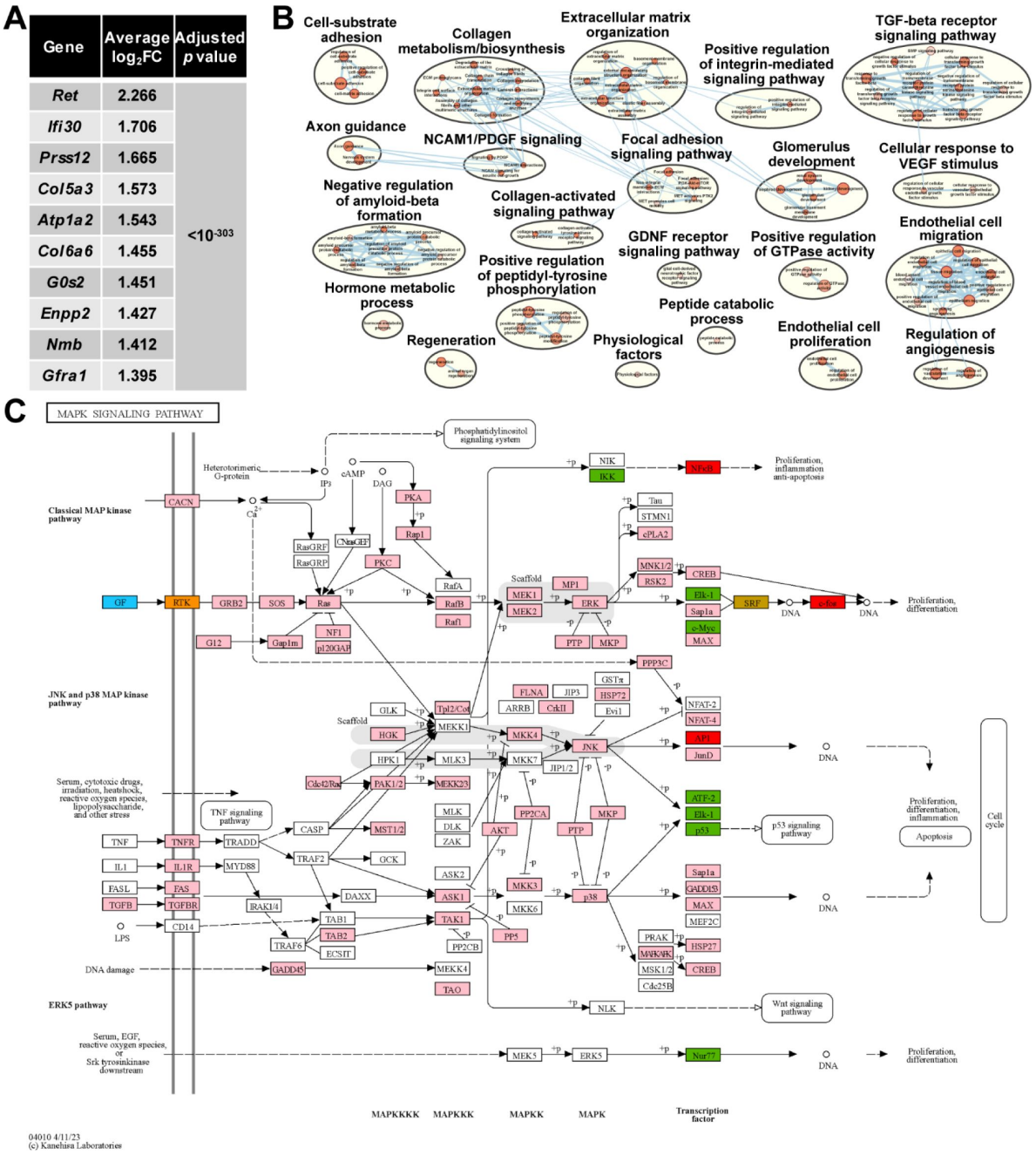

Figure 3—figure supplement 1.

Involvement of GDNF signaling pathway in the nerve injury-sensing mechanism by cluster 1 FAPs

(**A**) Top 10 genes specifically enriched in cluster 1 FAPs. P values were drawn from Wilcoxon rank sum test. (**B**) Results from g:Profiler showing pathways enriched using genes specifically enriched in cluster 1. (**C**) MAPK signaling pathway retrieved from KEGG, with color-coding to highlight relevant genes. Blue: GDNF ligand; orange: GDNF receptor Ret expressed in cluster 1; pink: downstream cascade genes expressed in clusters 1-3; red: transcription factors (TFs) commonly predicted to regulate upregulated genes in clusters 2 and 3; green: TFs predicted to regulate genes upregulated in cluster 2; gold: TFs predicted to regulate genes upregulated in cluster 3.

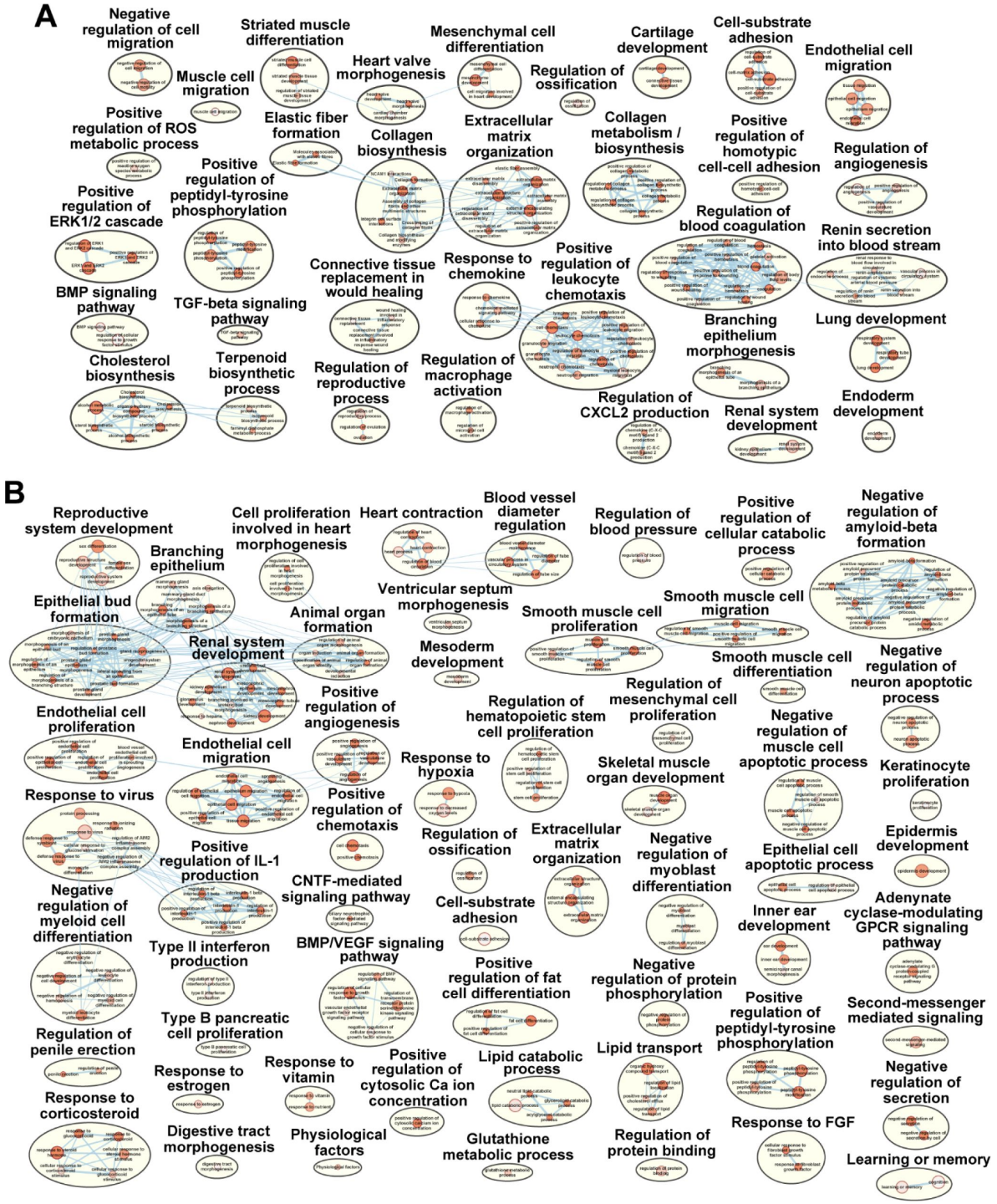

Figure 3—figure supplement 2.

Pathways enriched in the two activated clusters within nerve injury-affected FAPs

(**A**–**B**) Results from g:Profiler showing pathways enriched using genes specifically enriched in (A) cluster 2 or (B) cluster 3.

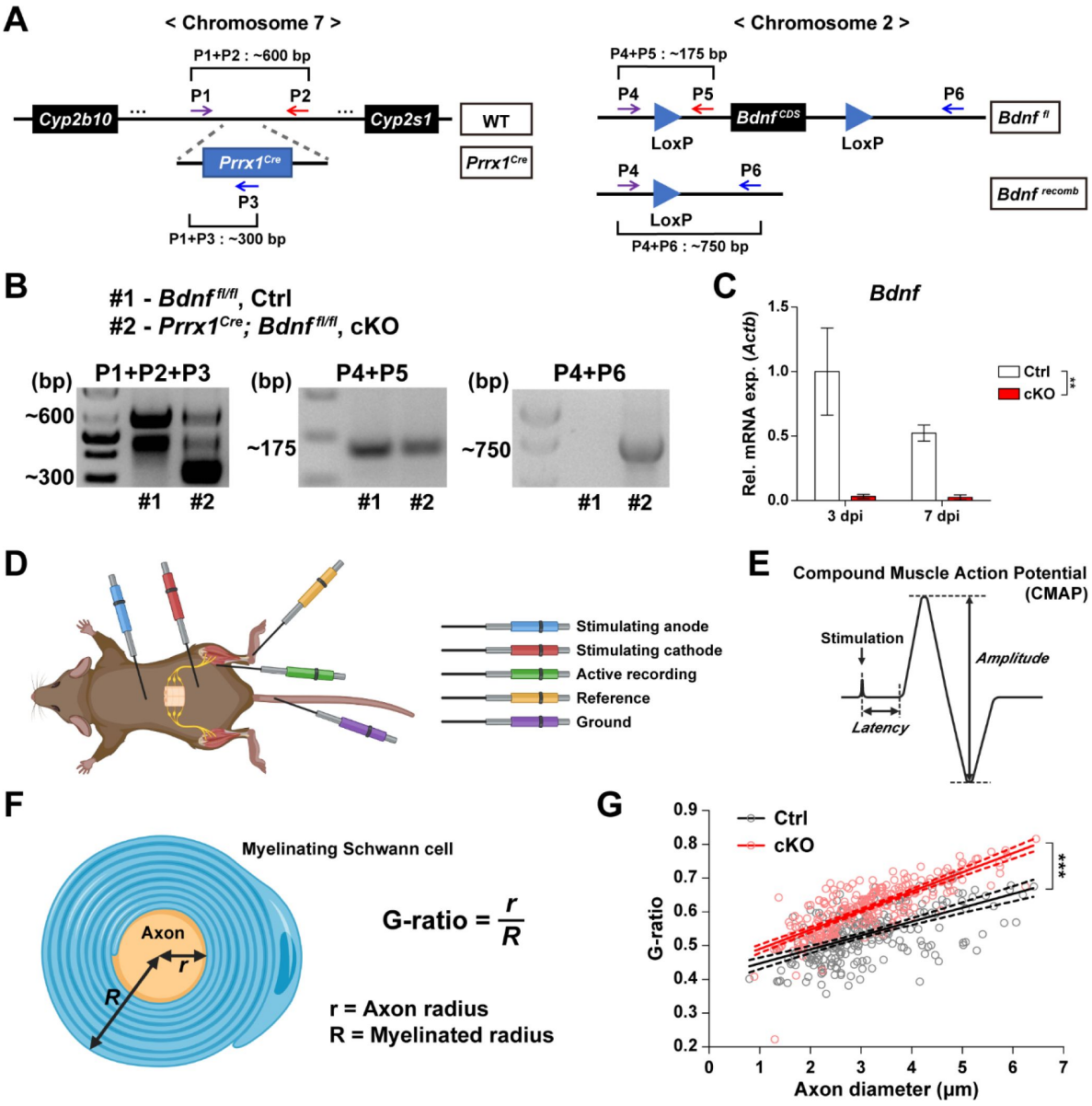

Figure 5—figure supplement 1.

Validation of cKO mice used in this study and methods used for analysis

(**A**) Genomic loci and structure of *Prrx1*^{Cre} and *Bdnf*^{fl} alleles labeled with primers used for genotyping and genomic DNA recombination validation. (**B**) Results from genotyping (left and middle) and genomic DNA recombination PCR (right). Genomic DNA recombination of the LoxP flanking sites in the cKO mice were confirmed using primers P4 and P6 shown in (A). (**C**) RT-qPCR results of *Bdnf* expression using FAPs isolated from either Ctrl or cKO mice at 3 or 7 days post SNC. n = 2; Two-way ANOVA. ** $p < 0.01$. (**D**) Scheme for CMAP measurement showing the positions of electrodes used. (**E**) Diagram of a typical CMAP graph along with amplitude and latency used for analysis. (**F**) Diagram depicting calculation of G-ratio. (**G**) Scatter plots with linear regressions displaying G-ratios (y-axis) in relation to axon diameters (x-axis). Solid lines are linear regressions and dotted lines represent error in 95% confidence level. ANCOVA, *** $p < 0.001$.

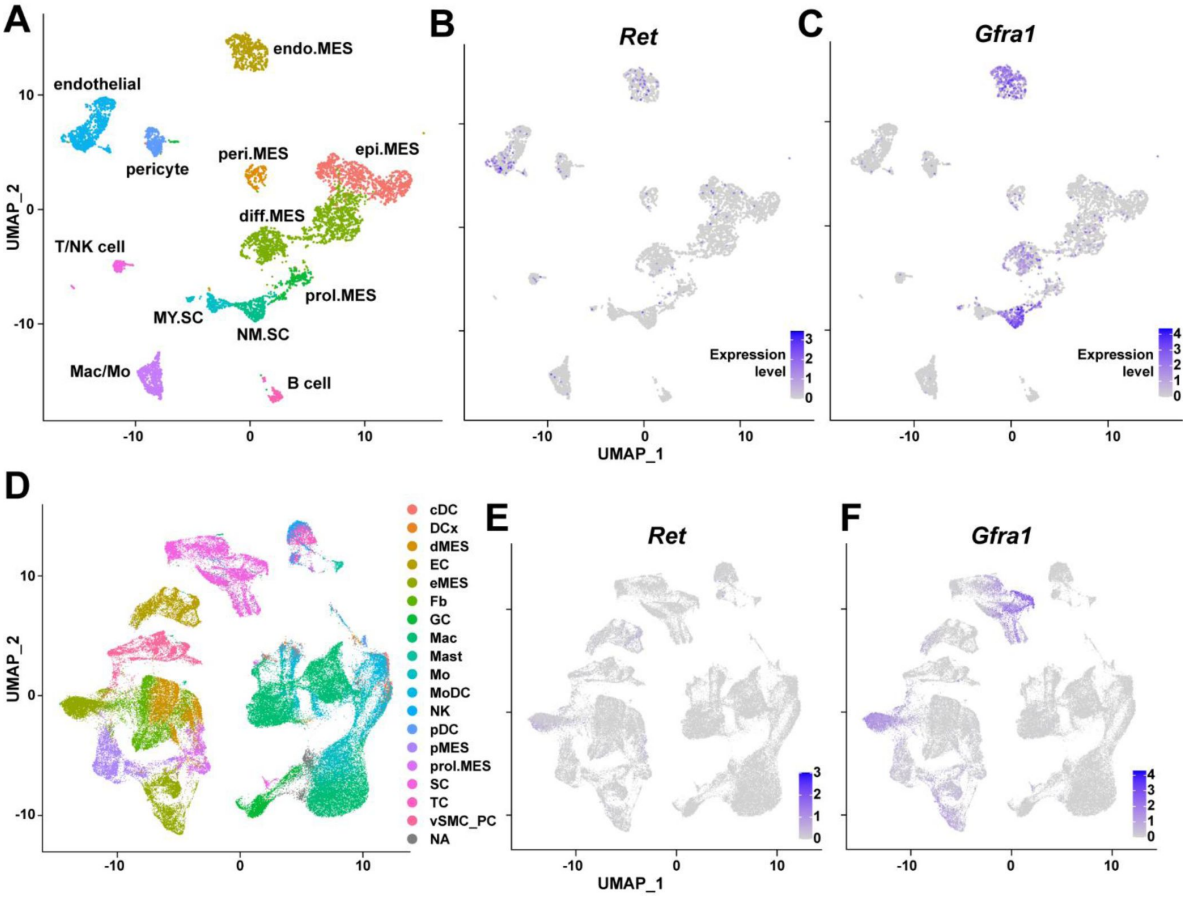

Supplemental figure 1.

Expression of GDNF receptor genes *Ret* and *Gfra1* in nerve-resident cells

(**A–C**) scRNA-seq data from Carr et al. (2019) and Toma et al. (2020) (accession numbers: GSM3408137, GSM3408139, GSM4423509, GSM4423506) were merged into a single Seurat object and visualized on UMAP plots. Cell types identified using markers listed by Toma et al. (2020) are shown in (A), and expression levels of (B) *Ret* and (C) *Gfra1* are displayed. epi.MES: epineurial mesenchymal cells; peri.MES: perineurial mesenchymal cells; endo.MES: endoneurial mesenchymal cells; diff.MES: differentiating mesenchymal cells; prol.MES: proliferating mesenchymal cells; NM.SC: non-myelinating Schwann cells; MY.SC: myelinating Schwann cells; Mac/Mo: macrophage/monocyte. (**D–F**) scRNA-seq data from Zhao et al. (2022) (accession number: GSE198582) were merged into a single Seurat object and visualized on UMAP plots. Cell types annotated by Zhao et al. (2022) are shown in (D), and expression levels of (E) *Ret* and (F) *Gfra1* are displayed. cDC: conventional dendritic cells; DCx: dendritic cells destined for homing; dMES: differentiating mesenchymal cells; EC: endothelial cells; eMES: endoneurial mesenchymal cells; Fb: fibroblasts; GC: granulocytes; Mac: macrophages; Mast: mast cells; Mo: monocytes; MoDC: monocyte-derived dendritic cells; NK: natural killer cells; pDC: plasmocytoid dendritic cells; pMES: perineurial mesenchymal cells; prol.MES: proliferating mesenchymal cells; SC: Schwann cells; TC: T cells; vSMC_PC: vascular smooth muscle cells/pericytes; NA: not applicable.

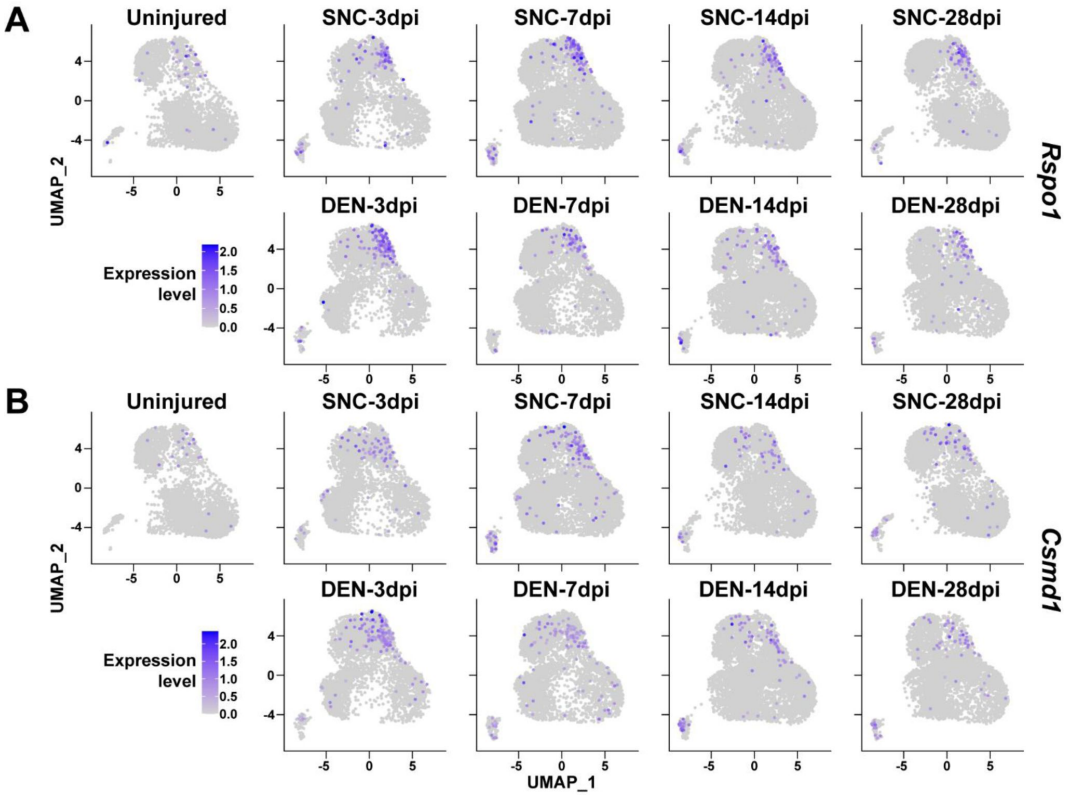

Supplemental figure 2.

Expression of nerve injury-induced, cluster-specific genes in FAPs

(**A**–**B**) Expressions of (A) *Rspo1* and (B) *Csmd1* shown on UMAP plots, separated by samples. scRNA-seq data obtained in this study were used.

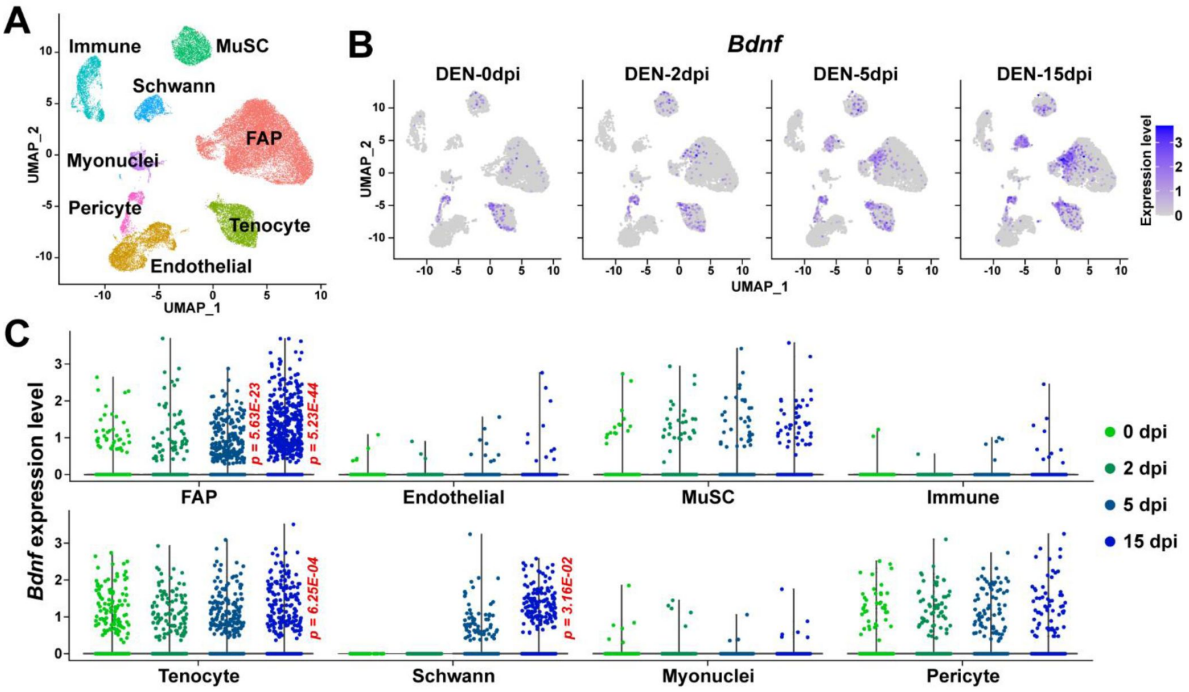

Supplemental figure 3.

Expression of *Bdnf* in muscle-resident mononuclear cells affected by denervation

(**A**) UMAP plot showing data from Nicoletti et al. (2023) labeled by cell types identified. (**B**) Expression pattern of *Bdnf* in data from Nicoletti et al. (2023) shown on UMAP plots, separately by days post denervation. (**C**) Expression of *Bdnf* in each cell type on different days post denervation displayed in violin plots. P values were calculated by comparing each injury-affected cells' expression levels versus its uninjured state (0 dpi). Only significant p values are shown. Wilcoxon rank sum test.

Key TF	Adjusted P value	List of overlapped genes
Jun	0.000114	Timp1, C1qtnf3, Plaur, Slc39a14, Mmp3, Itga5, Serpine1, Tgfb1, Mmp19, Ccl2, Slc8a1, Plau
Smad3	0.000399	Serpine1, Plau, Nedd9, Acta2, Ccl2, Tagln, Enpp1
Msx2	0.00464	Lss, Enpp1, Tagln, Alpl
Smad1	0.00579	Runx1, Col4a1, Col4a2, Tnfrsf11b
Ppard	0.00579	Angptl4, Tgfb1, Insig1
Sp1	0.00579	Acta2, Trf, Serpine1, Plaur, Lgals1, Mgp, Ccl2, Nes, Adcyap1r1, Itga5, Bmp4, Notch1, Skil
Fos	0.0149	Tgfb1, Bdnf, Tslp, Plau, Pdpn
Tgfb1i1	0.0149	Ccl2, Tgfb1
Srf	0.0185	Tagln, Barx2, Acta2
Id3	0.0298	Notch1, Alpl
Nfkb1	0.0298	Mmp3, Tgfb1, Dmp1, Pla2g4a, Il15, Egr2, Plaur, Ppp1r13l, Ccl2
Junb	0.034	Plau, Serpine1
Pparg	0.034	Serpine1, Muc1, Angptl4, C1qtnf3
Nfkb2	0.0362	Hif1a, Dmp1
Id1	0.0382	Thbs1, Alpl
Runx2	0.0382	Alpl, Mgp, Thbs1, Enpp1
Arntl	0.0382	Cxcl5, Bhlhe41
Msx1	0.0382	Tagln, Bmp4
Nr4a2	0.0382	Tnc, Gch1
Ets1	0.0388	Timp1, Mmp3, Ccl2, Bmp4
Prox1	0.0465	Pdpn, Notch1
Bcl3	0.0465	Runx1, Tnfrsf12a
Clock	0.0465	Serpine1, Bhlhe41
Etv4	0.0465	Mmp3, Plau

Supplemental table 1.

Results from TRRUST showing transcription factors predicted to regulate genes specifically enriched in cluster 2

Genes known to be regulated by each transcription factor is listed.

Key TF	Adjusted P value	List of overlapped genes
Nfkb1	1.64E-05	Cxcl10, Tnfsf13b, Cebpa, Apoe, Cxcl1, Il12a, Myc, Vcam1, Tnf, Sox9, Plin2, Rel, Igf2bp2, Birc3, Hmox1, Nfkbiz, Bcl2
Cebpb	0.000206	Bcl2, Myc, Mafb, Cebpa, Btg2, Serpine1, Socs3
Sp1	0.000206	Ces1d, Myc, Mgarp, Serpine1, Sirt1, Cebpd, Egr1, Apoe, Cebpa, Slc2a3, Socs3, Adcyap1r1, Tnf, Ar, Lpl, Bmp4, Igfbp3
Dlx5	0.000206	Wnt5a, Alpl, Myc, Igfbp3
Stat3	0.000206	Mt1, Il12a, Pnp, Socs3, Bcl2, Cebpd, Egr1, Tnf, Myc
Rela	0.000206	Tnfsf13b, Myc, Vcam1, Igf2bp2, Birc3, Pgf, Sox9, Cxcl10, Apoe, Tnf, Bcl2
Stat1	0.000336	Cxcl9, Egr1, Mt1, Socs3, Cebpd, Cxcl10
Id1	0.000336	Thbs1, Alpl, Rel, Tnf
Crebbp	0.000876	Socs3, Fosb, Tnf, Hmox1, Bcl2, Mt1
Rel	0.00115	Cebpd, Birc3, Il12a, Tnf, Myc
Jun	0.00119	Plin2, Cebpd, Cxcl1, Serpine1, Hmox1, Aldh1a1, Tnf, Sirt1, Socs3, Plau
Hnf1b	0.00135	Mafb, Pde4c, Socs3
Hif1a	0.00324	Mt1, Cited2, Hmox1, Serpine1
Tfap2a	0.00381	Apoe, Cebpa, Meis1
Trp53	0.00595	Btg2, Thbs1, Hmox1, Bcl2, Mt1, Agtr1a, Myc, Serpine1, Egr1, Pappa
Ikbkb	0.00595	Cxcl9, Cxcl10, Tnf
Epas1	0.00678	Serpine1, Cited2, Vcam1
Ppara	0.00678	Cebpa, Lpl, Cebpd, Serpine1, Bcl2
Twist1	0.00781	Fgf10, Sox9, Tnf, Mme
Smad3	0.00809	Serpine1, Plau, Sirt1, Tnfsf13b, Myc
Bcl3	0.00899	Tnf, Cxcl10, Ubc
Atf2	0.0104	Sox9, Cebpa, Tnf
Fos	0.0127	Socs3, Tslp, Mt1, Plau, Egr1
Etv2	0.0146	Sox9, Plau
Mtf1	0.0146	Pgf, Mt1
Rbl1	0.0146	Myc, Alpl
Ctnnb1	0.0167	Bmp4, Isl1, Myc, Tbx3, Gja1
Elk1	0.0181	Hmox1, Egr1
Fosl1	0.0181	Thbs1, Thbs2
Dnmt3a	0.0209	Vtn, Mt1
Foxg1	0.0209	Ebf3, Serpine1
Id3	0.0209	Vcam1, Alpl
Tbx1	0.0209	Ripply3, Fgf10
Egr1	0.0225	Tnf, Serpine1, Thbs1, Nr4a1, Il12a
Irf1	0.0225	Cxcl10, Il12a, Tnf
Foxo3	0.0225	Socs3, Sirt1
Gfi1b	0.0225	Meis1, Socs3
Junb	0.0225	Plau, Serpine1
Ncoa3	0.0225	Igfbp3, Tbx3
Foxo1	0.0242	Bcl2l11, Egr1, Lpl, Alpl

Supplemental table 2.

Results from TRRUST showing transcription factors predicted to regulate genes specifically enriched in cluster 3

Genes known to be regulated by each transcription factor is listed.

Myc	0.0242	Myc, Cebpd, Bcl2, Zfp36
Pparg	0.0246	Serpine1, Plin2, Egr1, Hmox1
Nfkb2	0.0246	Myc, Rel
Nr4a1	0.0246	Serpine1, Ar
Nfe2l2	0.0278	Bcl2, Hmox1, Sult1e1, Mt1
Id2	0.0278	Alpl, Zbtb16
Klf5	0.0278	Egr1, Serpine1
Creb1	0.0312	Bcl2, Nfkbiz, Slc2a3
Runx2	0.0336	Alpl, Thbs1, Hbegf, Sox9
Ets1	0.0369	Egr1, Hmox1, Nr2f1, Bmp4
Ep300	0.0382	Tnfsf13b, Mt1, Hmox1, Socs3
Usf2	0.04	Hmox1, Mt1
Mecp2	0.0496	Slc2a3, Igfbp3
Stat6	0.0496	Tnf, Egr1

Supplemental table 2. (continued)

Gene	Secreted	GO term related to neuron/glial cell regulation	Exclusive expression in activated FAPs
Bdnf	O	O	O
Apoe	O	O	X
Ccl2	O	O	X
Tgfb1	O	O	X
Tnf	O	O	X
Vcam1	O	O	X
Dmp1	O	X	O
C1qtnf3	O	X	X
Cxcl1	O	X	X
Cxcl10	O	X	X
Il12a	O	X	X
Il15	O	X	X
Mmp19	O	X	X
Mmp3	O	X	X
Plau	O	X	X
Plaur	O	X	X
Serpine1	O	X	X
Timp1	O	X	X
Tnfsf13b	O	X	X
Tslp	O	X	X
Bcl2	X	O	X
Egr1	X	O	X
Egr2	X	O	X
Hif1a	X	O	X
Hmox1	X	O	X
Igf2bp2	X	O	X
Mt1	X	O	X
Myc	X	O	X
Rel	X	O	X
Sirt1	X	O	X
Sox9	X	O	X
Aldh1a1	X	X	X
Birc3	X	X	X
Cebpa	X	X	X
Cebpd	X	X	X
Itga5	X	X	X
Nfkbiz	X	X	X
Pdpn	X	X	X
Pla2g4a	X	X	X
Plin2	X	X	X
Ppp1r13l	X	X	X
Slc39a14	X	X	X
Slc8a1	X	X	X
Socs3	X	X	X

Supplemental table 3.

Categorization of genes predicted to be regulated by transcription factors that act downstream of the GDNF signaling pathway

Note that only *Bdnf* fits into all three criteria.

No.	Primer	Usage	Sequence (5' to 3')
1	Prrx1Cre_com_R (P1)	Genotyping PCR	TAG TGA AGT GGA AGT TCC TGG
2	Prrx1Cre_WT_F (P2)	Genotyping PCR	CAG TTC CTA CCC TGA TTT CC
3	Prrx1Cre_Tg_F (P3)	Genotyping PCR	GAT CAT AAT CAG CCA TAC CAC
4	Bdnf_flox_F (P4)	Genotyping PCR	TGT GAT TGT GTT TCT GGT GAC
5	Bdnf_flox_R (P5)	Genotyping PCR	CGG TTT CTA AGC AAG TGA ACA
6	Bdnf_recomb_R (P6)	Genotyping PCR	GAA ATT TTC TCC ATC CCT ACT CCG GG
7	Cre_F	Genotyping PCR	GCA TTA CCG GTC GAT GCA ACG AGT GAT GAG
8	Cre_R	Genotyping PCR	GAG TGA ACG AAC CTG GTC GAA ATC AGT GCG
9	Rosa-tdT_WT_F	Genotyping PCR	AAG GGA GCT GCA GTG GAG TA
10	Rosa-tdT_WT_R	Genotyping PCR	CCG AAA ATC TGT GGG AAG TC
11	Rosa-tdT_Tg_F	Genotyping PCR	GGC ATT AAA GCA GCG TAT CC
12	Rosa-tdT_Tg_R	Genotyping PCR	CTG TTC CTG TAC GGC ATG G
13	Actb_qF	RT-qPCR	CCT CCC TGG AGA AGA GCT ATG
14	Actb_qR	RT-qPCR	TTA CGG ATG TCA ACG TCA CAC
15	Ret_qF	RT-qPCR	CCA GGG CTT CCC AAT CAG TT
16	Ret_qR	RT-qPCR	TTC CAA ACT CGC CTT CTC CC
17	Gfra1_qF	RT-qPCR	CAC TCC TGG ATT TGC TGA TGT
18	Gfra1_qR	RT-qPCR	AGT GTG CGG TAC TTG GTG C
19	Gdnf_qF	RT-qPCR	TCG GCC GAG ACA ATG TAT GA
20	Gdnf_qR	RT-qPCR	CAA CAT GCC TGG CCT ACT TTG
21	Bdnf_qF	RT-qPCR	AAG GAC GCG GAC TTG TAC AC
22	Bdnf_qR	RT-qPCR	CGC TAA TAC TGT CAC ACA CGC

Supplemental table 4.

Primers used in this study for genotyping PCR or RT-qPCR

References

Airaksinen MS, Saarma M (2002) **The GDNF family: signalling, biological functions and therapeutic value** *Nat Rev Neurosci* **3**:383–94 https://doi.org/10.1038/nrn812

Arthur-Farraj PJ *et al.* (2012) **c-Jun reprograms Schwann cells of injured nerves to generate a repair cell essential for regeneration** *Neuron* **75**:633–47 https://doi.org/10.1016/j.neuron.2012.06.021

Aurora AB, Olson EN (2014) **Immune modulation of stem cells and regeneration** *Cell Stem Cell* **15**:14–25 https://doi.org/10.1016/j.stem.2014.06.009

Bakooshli MA, Wang YX, Monti E, Su S, Kraft P, Nalbandian M, Alexandrova L, Wheeler JR, Vogel H, Blau HM (2023) **Regeneration of neuromuscular synapses after acute and chronic denervation by inhibiting the gerozyme 15-prostaglandin dehydrogenase** *Science Translational Medicine* **15** https://doi.org/10.1126/scitranslmed.adg1485

Baydyuk M, Xu B (2014) **BDNF signaling and survival of striatal neurons** *Front Cell Neurosci* **8** https://doi.org/10.3389/fncel.2014.00254

Buttner R, Schulz A, Reuter M, Akula AK, Mindos T, Carlstedt A, Riecken LB, Baader SL, Bauer R, Morrison H (2018) **Inflammaging impairs peripheral nerve maintenance and regeneration** *Aging Cell* **17** https://doi.org/10.1111/acel.12833

Carr MJ, Toma JS, Johnston APW, Steadman PE, Yuzwa SA, Mahmud N, Frankland PW, Kaplan DR, Miller FD (2019) **Mesenchymal Precursor Cells in Adult Nerves Contribute to Mammalian Tissue Repair and Regeneration** *Cell Stem Cell* **24**:240–256 https://doi.org/10.1016/j.stem.2018.10.024

Chung T, Prasad K, Lloyd TE (2014) **Peripheral neuropathy: clinical and electrophysiological considerations** *Neuroimaging Clin N Am* **24**:49–65 https://doi.org/10.1016/j.nic.2013.03.023

Contreras O, Rebolledo DL, Oyarzun JE, Olguin HC, Brandan E (2016) **Connective tissue cells expressing fibro/adipogenic progenitor markers increase under chronic damage: relevance in fibroblast-myofibroblast differentiation and skeletal muscle fibrosis** *Cell Tissue Res* **364**:647–660 https://doi.org/10.1007/s00441-015-2343-0

Contreras O, Rossi FMV, Theret M (2021) **Origins, potency, and heterogeneity of skeletal muscle fibro-adipogenic progenitors-time for new definitions** *Skelet Muscle* **11** https://doi.org/10.1186/s13395-021-00265-6

De Micheli AJ, Laurilliard EJ, Heinke CL, Ravichandran H, Fraczek P, Soueid-Baumgarten S, De Vlaminck I, Elemento O, Cosgrove BD (2020) **Single-Cell Analysis of the Muscle Stem Cell Hierarchy Identifies Heterotypic Communication Signals Involved in Skeletal Muscle Regeneration** *Cell Rep* **30**:3583–3595 https://doi.org/10.1016/j.celrep.2020.02.067

Doerflinger NH, Macklin WB, Popko B (2003) **Inducible site-specific recombination in myelinating cells** *Genesis* **35**:63–72 https://doi.org/10.1002/gene.10154

English AW, Liu K, Nicolini JM, Mulligan AM, Ye K (2013) **Small-molecule trkB agonists promote axon regeneration in cut peripheral nerves** *Proc Natl Acad Sci U S A* **110**:16217–22 https://doi.org/10.1073/pnas.1303646110

Fielder GC, Yang TW, Razdan M, Li Y, Lu J, Perry JK, Lobie PE, Liu DX (2018) **The GDNF Family: A Role in Cancer?** *Neoplasia* **20**:99–117 https://doi.org/10.1016/j.neo.2017.10.010

Forese MG, Pellegatta M, Canevazzi P, Gullotta GS, Podini P, Rivellini C, Previtali SC, Bacigaluppi M, Quattrini A, Taveggia C (2020) **Prostaglandin D2 synthase modulates macrophage activity and accumulation in injured peripheral nerves** *Glia* **68**:95–110 https://doi.org/10.1002/glia.23705

Ghosh A, Carnahan J, Greenberg ME (1994) **Requirement for BDNF in activity-dependent survival of cortical neurons** *Science* **263**:1618–1623 https://doi.org/10.1126/science.7907431

Goebbels S *et al.* (2010) **Elevated phosphatidylinositol 3,4,5-trisphosphate in glia triggers cell-autonomous membrane wrapping and myelination** *J Neurosci* **30**:8953–64 https://doi.org/10.1523/JNEUROSCI.0219-10.2010

Gonzalez D, Contreras O, Rebolledo DL, Espinoza JP, van Zundert B, Brandan E (2017) **ALS skeletal muscle shows enhanced TGF-beta signaling, fibrosis and induction of fibro/adipogenic progenitor markers** *PLoS One* **12** https://doi.org/10.1371/journal.pone.0177649

Grinsell D, Keating CP (2014) **Peripheral nerve reconstruction after injury: a review of clinical and experimental therapies** *Biomed Res Int* **2014** https://doi.org/10.1155/2014/698256

Hammarberg H, Piehl F, Cullheim S, Fjell J, Hokfelt T, Fried K (1996) **GDNF mRNA in Schwann cells and DRG satellite cells after chronic sciatic nerve injury** *NeuroReport* **7**:857–860 https://doi.org/10.1097/00001756-199603220-00004

Han H *et al.* (2018) **TRRUST v2: an expanded reference database of human and mouse transcriptional regulatory interactions** *Nucleic Acids Res* **46**:D380–D386 https://doi.org/10.1093/nar/gkx1013

Hann S-H, Kim S-Y, Kim Y-L, Jo Y-W, Kang J-S, Park H, Choi S-Y, Kong Y-Y (2023) **Depletion of SMN Protein in Mesenchymal Progenitors Impairs the Development of Bone and Neuromuscular Junction in Spinal Muscular Atrophy** *eLife Sciences Publications, Ltd* https://doi.org/10.7554/elife.92731.1

Hanz S *et al.* (2003) **Axoplasmic importins enable retrograde injury signaling in lesioned nerve** *Neuron* **40**:1095–1104 https://doi.org/10.1016/s0896-6273(03)00770-0

Hao Y *et al.* (2021) **Integrated analysis of multimodal single-cell data** *Cell* **184**:3573–3587 https://doi.org/10.1016/j.cell.2021.04.048

Heredia JE, Mukundan L, Chen FM, Mueller AA, Deo RC, Locksley RM, Rando TA, Chawla A (2013) **Type 2 innate signals stimulate fibro/adipogenic progenitors to facilitate muscle regeneration** *Cell* **153**:376–88 https://doi.org/10.1016/j.cell.2013.02.053

Hoke A, Gordon T, Zochodne DW, Sulaiman OA (2002) **A decline in glial cell-line-derived neurotrophic factor expression is associated with impaired regeneration after long-term Schwann cell denervation** *Exp Neurol* **173**:77–85 https://doi.org/10.1006/exnr.2001.7826

Jing S, Wen D, Yu Y, Holst PL, Luo Y, Fang M, Tamir R, Antonio L, Hu Z, Cupples R (1996) **GDNF–induced activation of the ret protein tyrosine kinase is mediated by GDNFR-α, a novel receptor for GDNF** *Cell* **85**:1113–1124

Joe AW, Yi L, Natarajan A, Le Grand F, So L, Wang J, Rudnicki MA, Rossi FM (2010) **Muscle injury activates resident fibro/adipogenic progenitors that facilitate myogenesis** *Nat Cell Biol* **12**:153–63 https://doi.org/10.1038/ncb2015

Joseph NM, Mukouyama YS, Mosher JT, Jaegle M, Crone SA, Dormand EL, Lee KF, Meijer D, Anderson DJ, Morrison SJ (2004) **Neural crest stem cells undergo multilineage differentiation in developing peripheral nerves to generate endoneurial fibroblasts in addition to Schwann cells** *Development* **131**:5599–612 https://doi.org/10.1242/dev.01429

Julier Z, Park AJ, Briquez PS, Martino MM (2017) **Promoting tissue regeneration by modulating the immune system** *Acta Biomater* **53**:13–28 https://doi.org/10.1016/j.actbio.2017.01.056

Kalinski AL *et al.* (2020) **Analysis of the immune response to sciatic nerve injury identifies efferocytosis as a key mechanism of nerve debridement** *Elife* **9** https://doi.org/10.7554/eLife.60223

Kanehisa M, Furumichi M, Sato Y, Kawashima M, Ishiguro-Watanabe M (2023) **KEGG for taxonomy-based analysis of pathways and genomes** *Nucleic Acids Res* **51**:D587–D592 https://doi.org/10.1093/nar/gkac963

Kim JH *et al.* (2022) **Bap1/SMN axis in Dpp4+ skeletal muscle mesenchymal cells regulates the neuromuscular system** *JCI Insight* **7** https://doi.org/10.1172/jci.insight.158380

Kolberg L, Raudvere U, Kuzmin I, Adler P, Vilo J, Peterson H (2023) **g:Profiler-interoperable web service for functional enrichment analysis and gene identifier mapping (2023 update)** *Nucleic Acids Res* **51**:W207–W212 https://doi.org/10.1093/nar/gkad347

Kucera M, Isserlin R, Arkhangorodsky A, Bader GD (2016) **AutoAnnotate: A Cytoscape app for summarizing networks with semantic annotations** *F1000Res* **5** https://doi.org/10.12688/f1000research.9090.1

La Manno G *et al.* (2018) **RNA velocity of single cells** *Nature* **560**:494–498 https://doi.org/10.1038/s41586-018-0414-6

Leinroth AP, Mirando AJ, Rouse D, Kobayahsi Y, Tata PR, Rueckert HE, Liao Y, Long JT, Chakkalakal JV, Hilton MJ (2022) **Identification of distinct non-myogenic skeletal-muscle-resident mesenchymal cell populations** *Cell Rep* **39** https://doi.org/10.1016/j.celrep.2022.110785

Lemos DR, Babaeijandaghi F, Low M, Chang CK, Lee ST, Fiore D, Zhang RH, Natarajan A, Nedospasov SA, Rossi FM (2015) **Nilotinib reduces muscle fibrosis in chronic muscle injury by promoting TNF-mediated apoptosis of fibro/adipogenic progenitors** *Nat Med* **21**:786–94 https://doi.org/10.1038/nm.3869

Lieberman B, Kusi M, Hung CN, Chou CW, He N, Ho YY, Taverna JA, Huang THM, Chen CL (2021) **Toward uncharted territory of cellular heterogeneity: advances and applications of single-cell RNA-seq** *J Transl Genet Genom* **5**:1–21 https://doi.org/10.20517/jtgg.2020.51

Lin H, Ma X, Sun Y, Peng H, Wang Y, Thomas SS, Hu Z (2022) **Decoding the transcriptome of denervated muscle at single-nucleus resolution** *J Cachexia Sarcopenia Muscle* **13**:2102–2117 https://doi.org/10.1002/jcsm.13023

Liu L, Cheung TH, Charville GW, Rando TA (2015) **Isolation of skeletal muscle stem cells by fluorescence-activated cell sorting** *Nat Protoc* **10**:1612–24 https://doi.org/10.1038/nprot.2015.110

Logan M, Martin JF, Nagy A, Lobe C, Olson EN, Tabin CJ (2002) **Expression of Cre Recombinase in the developing mouse limb bud driven by a Prxl enhancer** *Genesis* **33**:77–80 https://doi.org/10.1002/gene.10092

Lukjanenko L *et al.* (2019) **Aging Disrupts Muscle Stem Cell Function by Impairing Matricellular WISP1 Secretion from Fibro-Adipogenic Progenitors** *Cell Stem Cell* **24**:433–446 https://doi.org/10.1016/j.stem.2018.12.014

Madaro L *et al.* (2018) **Denervation-activated STAT3-IL-6 signalling in fibro-adipogenic progenitors promotes myofibres atrophy and fibrosis** *Nat Cell Biol* **20**:917–927 https://doi.org/10.1038/s41556-018-0151-y

Magill CK, Tong A, Kawamura D, Hayashi A, Hunter DA, Parsadanian A, Mackinnon SE, Myckatyn TM (2007) **Reinnervation of the tibialis anterior following sciatic nerve crush injury: a confocal microscopic study in transgenic mice** *Exp Neurol* **207**:64–74 https://doi.org/10.1016/j.expneurol.2007.05.028

Maita KC, Garcia JP, Avila FR, Torres-Guzman RA, Ho O, Chini CCS, Chini EN, Forte AJ (2023) **Evaluation of the Aging Effect on Peripheral Nerve Regeneration: A Systematic Review** *J Surg Res* **288**:329–340 https://doi.org/10.1016/j.jss.2023.03.017

Malecova B *et al.* (2018) **Dynamics of cellular states of fibro-adipogenic progenitors during myogenesis and muscular dystrophy** *Nat Commun* **9** https://doi.org/10.1038/s41467-018-06068-6

Mallik A, Weir AI (2005) **Nerve conduction studies: essentials and pitfalls in practice** *J Neurol Neurosurg Psychiatry* **76**:ii23–31 https://doi.org/10.1136/jnnp.2005.069138

Merico D, Isserlin R, Stueker O, Emili A, Bader GD (2010) **Enrichment map: a network-based method for gene-set enrichment visualization and interpretation** *PLoS One* **5** https://doi.org/10.1371/journal.pone.0013984

Mueller M, Wacker K, Ringelstein EB, Hickey WF, Imai Y, Kiefer R (2001) **Rapid response of identified resident endoneurial macrophages to nerve injury** *Am J Pathol* **159**:2187–97 https://doi.org/10.1016/S0002-9440(10)63070-2

Murphy MM, Lawson JA, Mathew SJ, Hutcheson DA, Kardon G (2011) **Satellite cells, connective tissue fibroblasts and their interactions are crucial for muscle regeneration** *Development* **138**:3625–37 https://doi.org/10.1242/dev.064162

Nicoletti C, Wei X, Etxaniz U, D'Ercole C, Madaro L, Perera R, Puri PL (2023) **Muscle denervation promotes functional interactions between glial and mesenchymal cells through NGFR and NGF** *iScience* **26** https://doi.org/10.1016/j.isci.2023.107114

Nicoletti C, Wei X, Etxaniz U, Proietti D, Madaro L, Puri PL (2020) **scRNA-seq-based analysis of skeletal muscle response to denervation reveals selective activation of muscle-resident glial cells and fibroblasts** *Biorxiv* https://doi.org/10.1101/2020.12.29.424762

Oprescu SN, Yue F, Qiu J, Brito LF, Kuang S (2020) **Temporal Dynamics and Heterogeneity of Cell Populations during Skeletal Muscle Regeneration** *iScience* **23** https://doi.org/10.1016/j.isci.2020.100993

Ortega-Gomez A, Perretti M, Soehnlein O (2013) **Resolution of inflammation: an integrated view** *EMBO Mol Med* **5**:661–74 https://doi.org/10.1002/emmm.201202382

Oudega M, Hagg T (1999) **Neurotrophins promote regeneration of sensory axons in the adult rat spinal cord** *Brain Research* **818**:431–438

Painter MW *et al.* (2014) **Diminished Schwann cell repair responses underlie age-associated impaired axonal regeneration** *Neuron* **83**:331–343 https://doi.org/10.1016/j.neuron.2014.06.016

Parrinello S, Napoli I, Ribeiro S, Wingfield Digby P, Fedorova M, Parkinson DB, Doddrell RD, Nakayama M, Adams RH, Lloyd AC (2010) **EphB signaling directs peripheral nerve regeneration through Sox2-dependent Schwann cell sorting** *Cell* **143**:145–55 https://doi.org/10.1016/j.cell.2010.08.039

Proietti D *et al.* (2021) **Activation of skeletal muscle-resident glial cells upon nerve injury** *JCI Insight* **6** https://doi.org/10.1172/jci.insight.143469

Reimand J *et al.* (2019) **Pathway enrichment analysis and visualization of omics data using g:Profiler, GSEA, Cytoscape and Enrichment** *Map Nat Protoc* **14**:482–517 https://doi.org/10.1038/s41596-018-0103-9

Roberts EW *et al.* (2013) **Depletion of stromal cells expressing fibroblast activation protein-alpha from skeletal muscle and bone marrow results in cachexia and anemia** *J Exp Med* **210**:1137–51 https://doi.org/10.1084/jem.20122344

Saito Y, Chikenji TS, Matsumura T, Nakano M, Fujimiya M (2020) **Exercise enhances skeletal muscle regeneration by promoting senescence in fibro-adipogenic progenitors** *Nat Commun* **11** https://doi.org/10.1038/s41467-020-14734-x

Sariola H, Saarma M (2003) **Novel functions and signalling pathways for GDNF** *J Cell Sci* **116**:3855–62 https://doi.org/10.1242/jcs.00786

Scheib J, Hoke A (2013) **Advances in peripheral nerve regeneration** *Nat Rev Neurol* **9**:668–76 https://doi.org/10.1038/nrneurol.2013.227

Scheib JL, Hoke A (2016) **An attenuated immune response by Schwann cells and macrophages inhibits nerve regeneration in aged rats** *Neurobiol Aging* **45**:1–9 https://doi.org/10.1016/j.neurobiolaging.2016.05.004

Scott RW, Arostegui M, Schweitzer R, Rossi FMV, Underhill TM (2019) **Hic1 Defines Quiescent Mesenchymal Progenitor Subpopulations with Distinct Functions and Fates in Skeletal Muscle Regeneration** *Cell Stem Cell* **25**:797–813 https://doi.org/10.1016/j.stem.2019.11.004

Shannon P, Markiel A, Ozier O, Baliga NS, Wang JT, Ramage D, Amin N, Schwikowski B, Ideker T (2003) **Cytoscape: a software environment for integrated models of biomolecular interaction networks** *Genome Res* **13**:2498–504 https://doi.org/10.1101/gr.1239303

Takemura Y *et al.* (2012) **Brain-derived neurotrophic factor from bone marrow-derived cells promotes post-injury repair of peripheral nerve** *PLoS One* **7** https://doi.org/10.1371/journal.pone.0044592

Theret M, Rossi FMV, Contreras O (2021) **Evolving Roles of Muscle-Resident Fibro-Adipogenic Progenitors in Health, Regeneration, Neuromuscular Disorders, and Aging** *Front Physiol* **12** https://doi.org/10.3389/fphys.2021.673404

Toma JS, Karamboulas K, Carr MJ, Kolaj A, Yuzwa SA, Mahmud N, Storer MA, Kaplan DR, Miller FD (2020) **Peripheral Nerve Single-Cell Analysis Identifies Mesenchymal Ligands that Promote Axonal Growth** *eNeuro* **7** https://doi.org/10.1523/ENEURO.0066-20.2020

Treanor JJ, Goodman L, de Sauvage F, Stone DM, Poulsen KT, Beck CD, Gray C, Armanini MP, Pollock RA, Hefti F (1996) **Characterization of a multicomponent receptor for GDNF** *Nature* **382**:80–83

Trupp M *et al.* (1996) **Functional receptor for GDNF encoded by the c-ret proto-oncogene** *Nature* **381**:785–789 https://doi.org/10.1038/381785a0

Uezumi A, Fukada S, Yamamoto N, Takeda S, Tsuchida K (2010) **Mesenchymal progenitors distinct from satellite cells contribute to ectopic fat cell formation in skeletal muscle** *Nat Cell Biol* **12**:143–52 https://doi.org/10.1038/ncb2014

Uezumi A, Ikemoto-Uezumi M, Tsuchida K (2014) **Roles of nonmyogenic mesenchymal progenitors in pathogenesis and regeneration of skeletal muscle** *Front Physiol* **5** https://doi.org/10.3389/fphys.2014.00068

Uezumi A *et al.* (2021) **Mesenchymal Bmp3b expression maintains skeletal muscle integrity and decreases in age-related sarcopenia** *J Clin Invest* **131** https://doi.org/10.1172/JCI139617

Uezumi A *et al.* (2011) **Fibrosis and adipogenesis originate from a common mesenchymal progenitor in skeletal muscle** *J Cell Sci* **124**:3654–64 https://doi.org/10.1242/jcs.086629

Vallecillo-Garcia P *et al.* (2017) **Odd skipped-related 1 identifies a population of embryonic fibro-adipogenic progenitors regulating myogenesis during limb development** *Nat Commun* **8** https://doi.org/10.1038/s41467-017-01120-3

Verdú E, Ceballos D, Vilches JJ, Navarro X (2008) **Influence of aging on peripheral nerve function and regeneration** *Journal of the Peripheral Nervous System* **5**:191–208 https://doi.org/10.1111/j.1529-8027.2000.00026.x

Wagstaff LJ *et al.* (2021) **Failures of nerve regeneration caused by aging or chronic denervation are rescued by restoring Schwann cell c-Jun** *Elife* **10** https://doi.org/10.7554/eLife.62232

Wilhelm JC, Xu M, Cucoranu D, Chmielewski S, Holmes T, Lau KS, Bassell GJ, English AW (2012) **Cooperative roles of BDNF expression in neurons and Schwann cells are modulated by exercise to facilitate nerve regeneration** *J Neurosci* **32**:5002–9 https://doi.org/10.1523/JNEUROSCI.1411-11.2012

Wosczyna MN, Konishi CT, Perez Carbajal EE, Wang TT, Walsh RA, Gan Q, Wagner MW, Rando TA (2019) **Mesenchymal Stromal Cells Are Required for Regeneration and Homeostatic Maintenance of Skeletal Muscle** *Cell Rep* **27**:2029–2035 https://doi.org/10.1016/j.celrep.2019.04.074

Xiao J, Wong AW, Willingham MM, Kaasinen SK, Hendry IA, Howitt J, Putz U, Barrett GL, Kilpatrick TJ, Murray SS (2009) **BDNF exerts contrasting effects on peripheral myelination of NGF-dependent and BDNF-dependent DRG neurons** *J Neurosci* **29**:4016–22 https://doi.org/10.1523/JNEUROSCI.3811-08.2009

Xu P, Rosen KM, Hedstrom K, Rey O, Guha S, Hart C, Corfas G (2013) **Nerve injury induces glial cell line-derived neurotrophic factor (GDNF) expression in Schwann cells through purinergic signaling and the PKC-PKD pathway** *Glia* **61**:1029–40 https://doi.org/10.1002/glia.22491

Zhang JY, Luo XG, Xian CJ, Liu ZH, Zhou XF (2000) **Endogenous BDNF is required for myelination and regeneration of injured sciatic nerve in rodents** *European Journal of Neuroscience* **12**:4171–4180 https://doi.org/10.1111/j.1460-9568.2000.01312.x

Zheng J, Sun J, Lu X, Zhao P, Li K, Li L (2016) **BDNF promotes the axonal regrowth after sciatic nerve crush through intrinsic neuronal capability upregulation and distal portion protection** *Neurosci Lett* **621**:1–8 https://doi.org/10.1016/j.neulet.2016.04.006

Editors

Reviewing Editor
Moses Chao
New York University Langone Medical Center, New York, United States of America

Senior Editor
Sacha Nelson
Brandeis University, Waltham, United States of America

Reviewer #1 (Public Review):

In this manuscript, Yoo et al describe the role of a specialized cell type found in muscle, Fibro-adipogenic progenitors (FAPs), in promoting regeneration following sciatic nerve injury. Using single-cell transcriptomics, they characterize the expression profiles of FAPs at various times after nerve crush or denervation. Their results reveal that a population of these muscle-resident mesenchymal progenitors up-regulate the receptors for GDNF, which is secreted by Schwann cells following crush injury, suggesting that FAPs respond to this growth factor. They also find that FAPs increase expression of BDNF, which promotes nerve regeneration. The authors demonstrate FAP production of BDNF in vivo is upregulated in response to injection of GDNF and that conditional deletion of BDNF in FAPs results in delayed nerve regeneration after crush injury, primarily due to lagging remyelination. Finally, they also find reduced BDNF expression following crush injury in aged mice, suggesting a potential mechanism to explain the decrease in peripheral nerve regenerative capability in aged animals. These results are very interesting and novel and provide important insights into the mechanisms regulating peripheral nerve regeneration, which has important clinical implications for understanding and treating nerve injuries. However, there are a few concerns that the authors need to address.

Given that only a fraction of the FAPs express BDNF after injury, the authors need to demonstrate the specificity of the Prrx1-Cre for FAPs. This is particularly important because

muscle stem cell also express GDNF receptors (Fig. 3C & D) and myogenic progenitors/satellite cells produce BDNF after nerve injury (Griesbeck et al., 1995 (PMID 8531223); Omura et al., 2005 (PMID 16221288)). Moreover, as the authors point out, there are multipotent mesenchymal precursor cells in the nerve that migrate into the surrounding tissue following nerve injury and contribute to regeneration (Carr et al, PMID 30503141). Therefore, there are multiple possible sources of BDNF, highlighting the need to clearly demonstrate that FAP-derived BDNF is essential.

Similarly, the authors should provide some evidence that BDNF protein is produced by FAPs. All of their data for BDNF expression is based on mRNA expression and that appears to only be increased in a small subset of FAPs. Perhaps an immunostaining could be done to demonstrate up-regulation of BDNF in FAPs after injury.

The suggestion that Schwann cell-derived GDNF is responsible for up-regulation of BDNF in the FAPs is indirect, based largely on the data showing that injection of GDNF into the muscle is sufficient to up-regulate BDNF (Fig. 4F & G). However, to more directly connect the 2 observations in a causal way, the authors should inject a Ret/GDNF antagonist, such as a Ret-Fc construct, then measure the BDNF levels.

In assessing the regeneration after nerve crush, the authors focus on remyelination, for example, assessing CMAP and g-ratios. However, they should also quantify axon regeneration, which can be done distal to the crush injury at earlier time points, before the 6 weeks scored in their study. Evaluating axon regeneration, which occurs prior to remyelination, would be especially useful because BDNF can act on both Schwann cells, to promote myelination, and axons, enhancing survival and growth. They could also evaluate the stability of the neuromuscular junctions, particularly if a denervation was done with the conditional knock outs, although that may be a bit beyond the scope of this study.

https://doi.org/10.7554/eLife.97662.1.sa2

Reviewer #2 (Public Review):

Summary:

Yoo and colleagues studied the cellular mechanism allowing fibro-adipogenic progenitors (FAPs), muscle resident mesenchymal progenitors, to contribute to nerve regeneration upon regenerative injury. In addition to their expected role in the maintenance of muscle tissue, FAPs also contribute to the maturation and maintenance of neural tissue. After nerve injury, they prevent dying back loss of motor neurons. Consistently, muscle denervation activates FAPs, suggesting that FAPs can sense the injured distal peripheral nerve.

A transcriptomic database was established using flow cytometry protocols and single-cell RNA-seq. FAPs were isolated from sciatic nerve crush (SNC), considered a regenerative condition, and compared to a non-regenerative condition consisting of denervation-affected muscles (DEN) at different time points after injury: early (3 and 7 days post-injury, dpi) and late (14 and 28 dpi), when the regeneration process has started to resolve. Transcriptome changes of the nine different conditions were compared: non-injured, 3, 7, 14, and 28 days after injury. Bioinformatic analysis and other filters were applied, including UMAP plots, hierarchical clustering analysis using differentially expressed genes (DEGs), volcano plots, and RNA velocity analysis. In addition to most of the supplementary material, the first three and a half central figures consist of the analysis of the transcriptome changes comparing the different conditions. Overall, the data indicate similar DEGs after both types of injury at early stages. Still, just after SNC, the gene expression pattern reaches similar levels compared to non-injured, meaning the injured process is resolved. For example, the Interleukin6/Stat3 pathway is upregulated in both injury models but downregulated at 28 days just in SNC.

When focusing on the comparison between 28 dpi between both types of injury, it indicates a role of FAPs in the resolution of inflammation in SNC and participation of FAPs in fibrosis and inflammation in DEN at 28 dpi. Genes related to wound healing were enriched in both.

With the question in mind of how FAPs are sensing injury, the authors identified a subset of FAPs relevant to regeneration in the SNC model. The unsupervised clustering of FAPs cells considering the nine different types of samples resulted in seven clusters of FAPs. Cluster one was exclusive to non-injury animals or regenerated samples. Clusters two and three were exclusive to the early injured or denervated nerve, suggesting that cluster one senses injury and clusters two and three are derived from it. Among the highest DEGs in cluster one were the GDNF receptors Ret and Gfra1. It is known that GDNF is released by Schwann cells after nerve injury in the literature. Also, gene expression analysis in clusters two and three predicts RTK involvement and GDNF signaling. Altogether, transcriptomic data suggest that GDNF is the mechanism by which FAPs sense nerve injury.

On the other hand, they found BDNF expression limited to cluster two of injured FAPs, suggesting that FAPs respond to GDNF by secreting BDNF. Although the specific role of secreted BDNF by FAPs in nerve regeneration is unknown, BDNF is known to have a regenerative influence on injured sciatic nerves by promoting both axonal growth and myelination. Consistent with their hypothesis, the analysis of gene expression in Schwann cells (sorted using the Plp1CreER Rosatd tomato mouse) and FAPs after injury indicates an initial increase in GDNF gene expression in early time points after injury in Schwann cells, followed by increased expression of BDNF in FAPs. Using conditional knock-out of BDNF in low limb FAPs (Prrx1Cre; Bdnffl/fl), they were able to demonstrate that nerve regeneration is impaired in Prrx1Cre; Bdnffl/fl, by delayed myelinization of axons.

Strengths:

I found the article well-written and cleverly maximized the interpretation and analysis of single-cell transcriptome data. Their findings illuminate how growth factors allow communication between cells responding to injury to promote regeneration. I find the data generated by the authors sufficient to support their model and claims,

Weaknesses:

Although, I find the data the authors generated enough for their claims. I do see them as relatively poor, and a complementary analysis of protein expression would strengthen the paper through immunostaining of the different genes mentioned for FAPs and Schwann cells. The model is entirely supported by measuring mRNA levels and negative regulation of gene expression in specific cells. Additionally, what happens to the structure of the neuromuscular junction after regeneration when GDNF or BDNF expression is reduced? The determination of decreasing levels of FAPs BDNF mRNA during aging is interesting; is the gain of BDNF expression in FAPs reverting the phenotype?

https://doi.org/10.7554/eLife.97662.1.sa1

Reviewer #3 (Public Review):

Summary:

The manuscript by Kyusang Yoo et al. "Muscle-resident mesenchymal progenitors sense and repair peripheral nerve injury via the GDNF-BDNF axis" investigates the role and mechanisms of fibro-adipogenic progenitors (FAPs), that are muscle-resident mesenchymal progenitors, in the maturation and maintenance of the neuromuscular system. There is earlier evidence that absence of FAPs or its functional decline with age cause smaller regenerated myofibers. Role of FAPs on peripheral nerve regeneration is very poorly studied.

This study has translational importance because traumatic injury to the peripheral nerve can cause lifelong paralysis of the injured limb.

This manuscript provides data indicating that GDNF-BDNF axis plays an important role in peripheral nerve regeneration and function.

Strengths:

Because the role of FAPs on peripheral nerve regeneration is very poorly studied this investigation is a major step towards understanding the mechanism on the role of FAPs. They use scRNA-seq, animal models, and cKO mice that is also important. This study has translational importance because traumatic injury to the peripheral nerve can cause lifelong paralysis of the injured limb.
This is an interesting and original study focusing on the role of FAPs and indicating that GDNF-BDNF axis plays an important role in peripheral nerve regeneration and function.

Weaknesses:

In Fig. 1 and 2 authors provide data on scRNA seq and this is important information reporting the finding of RET and GFRa1 transcripts in the subpopulation of FAP cells. However, authors provide no data on the expression of RET and GFRa1 proteins in FAP cells. Another problem is the lack of information showing that GDNF secreted by Schwann cells can activate RET and its down-stream signaling in FAP cells.
There is no direct experimental proof that GDNF activating GFRa1-RET signaling triggers BDNF upregulation In FAP cells.
The data that GDNF signaling is inducing the synthesis and secretion of BDNF is also not conclusive.

https://doi.org/10.7554/eLife.97662.1.sa0